2012-12-03

Necessary and Sufficient Informativity Conditions for Robust Network Reconstruction Using Dynamical Structure Functions

Vasu Nephi Chetty
Brigham Young University - Provo

Necessary and Sufficient Informativity Conditions for Robust Network Reconstruction Using Dynamical Structure Functions

Vasu Chetty

A thesis submitted to the faculty of
Brigham Young University
in partial fulfillment of the requirements for the degree of

Master of Science

Sean Warnick, Chair
Julianne Grose
Daniel Zappala

Department of Computer Science

Brigham Young University

December 2012

ABSTRACT

Necessary and Sufficient Informativity Conditions for Robust Network Reconstruction Using Dynamical Structure Functions

Vasu Chetty
Department of Computer Science, BYU
Master of Science

Dynamical structure functions were developed as a partial structure representation of linear time-invariant systems to be used in the reconstruction of biological networks. Dynamical structure functions contain more information about structure than a system's transfer function, while requiring less a priori information for reconstruction than the complete computational structure associated with the state space realization. Early sufficient conditions for network reconstruction with dynamical structure functions severely restricted the possible applications of the reconstruction process to networks where each input independently controls a measured state.

The first contribution of this thesis is to extend the previously established sufficient conditions to incorporate both necessary and sufficient conditions for reconstruction. These new conditions allow for the reconstruction of a larger number of networks, even networks where independent control of measured states is not possible.

The second contribution of this thesis is to extend the robust reconstruction algorithm to all reconstructible networks. This extension is important because it allows for the reconstruction of networks from real data, where noise is present in the measurements of the system.

The third contribution of this thesis is a Matlab toolbox that implements the robust reconstruction algorithm discussed above. The Matlab toolbox takes in input-output data from simulations or real-life perturbation experiments and returns the proposed Boolean structure of the network.

The final contribution of this thesis is to increase the applicability of dynamical structure functions to more than just biological networks by applying our reconstruction method to wireless communication networks. The reconstruction of wireless networks produces a dynamic interference map that can be used to improve network performance or interpret changes of link rates in terms of changes in network structure, enabling novel anomaly detection and security schemes.

Keywords: Realization theory, dynamical structure functions, informativity conditions, network reconstruction, network inference, system identification, dynamic interference maps, wireless networks, PAS Kinase pathway, chemical reaction networks, partial structure representation, linear time-invariant systems

ACKNOWLEDGMENTS

I would like to thank my wonderful wife, Leticia Chetty, for all her help and support. I would also like to thank all my colleagues in the IDeA Labs at Brigham Young University, especially Julius Adebayo, Anurag Rai, and Devon Harbaugh for all their ideas and contributions to this thesis. Finally, I would like to thank my thesis committee, my advisor Sean Warnick, Julianne Grose, and Daniel Zappala, and all our other contributors with our work in Dynamical Structure Functions, especially Ye Yuan and Jorge Goncalves.

Table of Contents

List of Figures

List of Tables

Chapter 1

Introduction

The problem of network reconstruction, also known as reverse engineering or network inference, is defined differently for varying applications. However, no matter what the application, the network reconstruction problem is the attempt to discover the underlying structure of a particular system, [1].

Network reconstruction in biological systems has been of recent interest in the systems biology community, [2], [3], [4], [5], [6], [7]. The network reconstruction process has aided biologists in understanding the interactions of systems at the molecular level. This improved knowledge has been essential for numerous applications, such as cancer research [8], weight control [9], and understanding the immune system response during bacterial infection [10].

For computer networks, both wired and wireless, the network reconstruction problem is the discovery of the network topology or the interference map associated with the network. The reconstruction problem has also been a topic of interest recently in the networking community, [11], [12], [13]. For this thesis we look specifically at the creation of dynamic interference maps for wireless networks. This representation of the network is useful for network management as well as improving security.

The first step in applying any network reconstruction algorithm for a given application is to ensure that we understand the notion of structure for the system. There are various views of the structure of a system. A complete view of the system's structure is defined in Section 1.3, and it uses differential equations to create a comprehensive model or blueprint of

the system detailing the physical interconnection of system components. Differing views of structure reflect different ways of simplifying the complete view of this blueprint.

In order to ensure that we can create these blueprints for the applications of wireless networks and biological systems, we begin by modeling them in Sections 1.1 and 1.2 using systems of differential equations. Given these models we are then equipped to discuss various views of structure in Section 1.3.

1.1 Modeling Wireless Networks

Modeling wireless networks as a system of differential equations is somewhat difficult because they are discrete event systems, where the dynamics of the system are determined by the choices of the sending nodes on when to send packets. In [14] it was shown that although wireless networks are discrete event systems, their equilibrium properties as well as the transition dynamics can be captured using differential equations.

The wireless network model captures carrier sensing and backoff behavior of the 802.11 MAC, meaning that a link is only active if no other links within a certain range, known as the carrier sensing range, is broadcasting. Packets sent to the MAC layer from TCP and IP are queued and sent as soon as possible, i.e. once no other links are broadcasting, leading the MAC to consume all available bandwidth. This results in instantaneous sending rates that are either zero or the full link speed. Since the instantaneous sending rate contained discontinuities, the average rate over a sliding window was considered. This smoothed the discontinuities of instantaneous rates and allowed for accurate modeling of rate dynamics with differential equations.

The wireless network is a link-based model, so each state in the model represents the state of a link, not that of a sender or receiver. We denote the normalized sending rate of link i as x_i and denote the buffer size as b_i. The rate of change in the buffer size is the difference between the rate of packet arrival and departure from the buffer, i.e. $\frac{db_i}{dt} = u_i - x_i$ where u_i is the rate at which packets are sent from higher layers to the MAC layer.

To determine how much bandwidth is available to link x_i, normalized rates are used to show the probability that a particular link is active at a given time. The bandwidth available to link i is the probability that none of the links are active which contend with link i.

Let X_i denote a Bernoulli random variable indicating whether link i is broadcasting, i.e., $P(X_i = 1) = x_i$ and $P(X_i = 0) = 1 - x_i$. Similarly, let $\bar{X}_i$ be a Bernoulli random variable indicating whether any link contending with link i is broadcasting. By the Law of Total Probability, the bandwidth available to link i is:

$$P(\bar{X}_i = 0) = P(X_i = 1)P(\bar{X}_i = 0 \,|\, X_i = 1) + P(X_i = 0)P(\bar{X}_i = 0 \,|\, X_i = 0). \tag{1.1}$$

Assuming that two contending links never broadcast concurrently we get $P(\bar{X}_i = 0 \,|\, X_i = 1) = 1$.We begin by assuming that link i is the only common link between cliques, before generalizing our results to the case when there are multiple common links between cliques. The probability that all links in clique j are silent given link i is silent is $1 - \frac{1}{1-x_i} \sum_{k \in (L_j \setminus i)} x_k$ where L_j is the set of links in clique j. The non-contending links between two overlapping cliques are independent after conditioning on the common links (here just link i). Then

$$P(\bar{X}_i = 0 \,|\, X_i = 0) = \prod_{j \in C_i} \left(1 - \frac{1}{1 - x_i} \sum_{k \in (L_j \setminus i)} x_k \right)$$

where C_i is the set of a maximal cliques containing link i. Combining these intermediate steps, (1.1) can be rewritten as

$$P(\bar{X}_i = 0) = x_i + (1 - x_i) \prod_{j \in C_i} \left(1 - \frac{1}{1 - x_i} \sum_{k \in (L_j \setminus i)} x_k \right)$$

To avoid wasting bandwidth, the available rate should only influence the dynamics for link i when there are buffered packets ready to be sent. A sigmoid function is used as a continuous approximation of the step function to ensure there are no discontinuities in

th dynamics, i.e., $\sigma(b) = \frac{1}{1+e^{-\alpha b}}$ where α dictates the slope of the sigmoid at zero. For our simulations, we let $\alpha = 1$.

The 802.11 MAC dictates short periods of mandatory silence following each transmission. In addition to fixed length delays, stations are required to wait for a period of random duration before transmitting. This is done to avoid collisions caused by multiple stations attempting to broadcast immediately following the end of a transmission. The random backoff time is chosen uniformly within a range known as the contention window. The combination of mandatory silence and the random backoff decreases the maximum achievable throughput. The proportion of achievable throughput for link i is denoted by $\beta_i \in (0, 1)$.

The overall dynamics for a topology having at most one common link between any two cliques are

$$\begin{aligned} \dot{b}_i =& u_i - x_i \\ \dot{x}_i =& -x_i + \beta_i \sigma(b_i) \left(x_i + (1 - x_i) \prod_{j \in C_i} \left(1 - \frac{\sum_{k \in L_j \setminus i} x_k}{1 - x_i} \right) \right). \end{aligned} \tag{1.2}$$

To generalize the result to allow for more overlap between cliques, let

$$O_i = \{i\} \cup \{j : \exists k, l,\ k \neq l,\ j \in L_k,\ j \in L_l, \text{ and } k, l \in C_i\}$$

denote the set of links common to multiple cliques in C_i. The union with $\{i\}$ ensures the model simplifies correctly in the case where link i belongs to a single clique. Allowing for this in the preceding development leads to the dynamics

$$\dot{b}_i = u_i - x_i \tag{1.3}$$

$$\dot{x}_i = -x_i + \beta_i \sigma(b_i) \left(x_i + \prod_{j \in O_i} (1 - x_j) \prod_{j \in C_i} \left(1 - \frac{\sum_{k \in L_j \setminus O_i} x_k}{1 - \sum_{k \in O_i \cap L_j} x_k} \right) \right).$$

Validation for this model can be found in [14], where Matlab simulations of various topologies compare favorably to the results of packet-level ns-3 simulations.

1.2 Modeling Biological Networks

Now that we've established how to model wireless networks using differential equations, we show how the same is possible for biological networks. First, we note that chemical reaction networks describe a sequence of elementary chemical reactions, which are collisions of reactant molecules that form certain products, absorbing and releasing energy in the process, [15], [16]. A simple example of an elementary reaction would be:

$$\mathrm{X} + \mathrm{Y} \xrightarrow{k_1} \mathrm{Z} \tag{1.4}$$

where X, Y, and Z are chemical species and $k_1 \in \mathbb{R}^+$ is a number characterizing how quickly or slowly the reaction takes place (small k_1 describes a slow reaction, while large k_1 describes a fast reaction). For this chemical reaction, a molecule of X combines with Y to generate a molecule Z at a rate of k_1. We call X and Y the *reactants*, and Z the *product* of the reaction.

Chemical kinetic equations can be represented by a series of differential equations by applying the law of mass action, which states that the rate of the forward reaction is proportional to the product of the concentrations of the reactants, each raised to the power of its coefficient in the balanced equation, [17]. It has been purported that the law of mass action may not hold if the medium is not "well-mixed," [16].

By applying the law of mass action, the chemical kinetics associated with the reaction Equation 1.4 can be represented mathematically as follows:

$$\begin{aligned} \dot{x} &= -k_1 xy \\ \dot{y} &= -k_1 xy \\ \dot{z} &= k_1 xy \end{aligned} \tag{1.5}$$

Note that there is a differential equation for each molecule, each defining how the concentration of a molecule in the elementary reaction step changes over time. Chemical concentrations of the chemical species X, Y, and Z are denoted by their lowercase counterparts x, y, and z, respectively, using the systems biology notation as in [16]. The equivalent in traditional chemistry is to denote the chemical concentrations using square brackets, so the chemical concentration for X would be denoted $[X]$.

If the reverse reaction of Equation 1.4 also occurred, $\mathrm{Z} \xrightarrow{k_2} \mathrm{X} + \mathrm{Y}$, then the series of differential equations representing these chemical reactions becomes:

$$\begin{aligned} \dot{x} &= -k_1 xy + k_2 z \\ \dot{y} &= -k_1 xy + k_2 z \\ \dot{z} &= k_1 xy - k_2 z \end{aligned} \tag{1.6}$$

The combination of Equation 1.4 with its reverse reaction can be simplified to the chemical kinetic equation:

$$\mathrm{X} + \mathrm{Y} \underset{k_2}{\overset{k_1}{\rightleftharpoons}} \mathrm{Z}$$

Chemical reactions often involve more than one of the same molecule. The different numbers of molecules that are necessary to form the desired compounds in various quantities are called the *stoichiometry* of the reaction. For example, the chemical reaction $2\,\mathrm{A} + 3\,\mathrm{B} \xrightarrow{k_3} \mathrm{C}$

has stoichiometry $2:3:1$ and is modeled by the series of differential equations:

$$\begin{aligned}\dot{a} &= -k_3 a^2 b^3 \\ \dot{b} &= -k_3 a^2 b^3 \\ \dot{c} &= k_3 a^2 b^3\end{aligned}$$

Using the above theory for chemical kinetics, we will now look at an example of a chemical reaction network, which is essentially the interactions between a set of elementary reaction steps.

Example 1. *Consider the following set of chemical reactions:*

$$\mathrm{A} + \mathrm{E} \xrightarrow{k_1} \mathrm{C} \underset{k_3}{\overset{k_2}{\rightleftharpoons}} 2\,\mathrm{B} + \mathrm{E}$$

Under mass-action assumptions, these reactions suggest the following chemical kinetics:

$$\begin{aligned}\dot{a} &= -k_1 ae \\ \dot{b} &= k_3 b^2 e - k_2 c \\ \dot{c} &= k_1 ae - k_3 b^2 e + k_2 c \\ \dot{e} &= -k_1 ae + k_3 b^2 e - k_2 c\end{aligned} \tag{1.7}$$

□

1.2.1 The Hill Equation

In order to complete our understanding of modeling biological systems using differential equations we now add a quick note on the Hill equation. The Hill equation was first proposed by A.V. Hill in 1910 in order to describe the equilibrium relationship between oxygen tension and the saturation of haemoglobin [18]. More recently the Hill qeuation has been used for other applications, such as describing the drug concentration-effect relationship, [19].

The general form of the Hill equation is a three parameter equation describing the relationship between two variables, x (the independent variable) and y (the dependent variable):

$$y = \frac{y_{max} x^{\alpha}}{c^{\alpha}}$$

the three parameters are y_{max}, c, and α, [19].

Since there are many possible uses of the Hill equation, we will focus now on just two specific uses of the Hill equation that are prevalent today. The Michaelis-Menten equation, [20], is a special example of the Hill Equation and describes the relationship between the velocity of a reaction, v, and the concentration of a substrate, s, with the following expression:

$$v = \frac{(V_{max})s}{K_m + s}$$

where v is the initial velocity, V_{max} is the maximum reaction rate, s is the substrate concentration and K_m is concentration of substrate at which the rate of the enzymatic reaction is half V_{max}, [19].

Another important application of the Hill equation is with regards to physiochemical equilibrium. Let us consider the notion of a single equilibrium reaction between two molecules, L and M, and their combination, LM. This can be denoted using chemical reaction kinetics as

$$\mathrm{L} + \mathrm{M} \rightleftharpoons \mathrm{LM}.$$

The Hill equation defining y, the ratio of molecules of L that have reacted, is:

$$y = \frac{m}{K_D + m}$$

where m is the concentration of the molecule M and K_D represents the concentration of$M$ for which y is equal to 0.5 (i.e. $\frac{y_{max}}{2}$).

This result can be extended for multiple binding patterns, such as multiple molecules of a ligand binding to a receptor, by considering the following equilibrium:

$$\mathrm{L}_n + \mathrm{nM} \rightleftharpoons \mathrm{L}_n\mathrm{M}.$$

The corresponding Hill equation then becomes:

$$y_n = \frac{m^n}{K_n + m^n}.$$

1.3 Network Structure Representations

Thus we have shown that we can produce a series of differential equations representing the the behavior of links in a wireless network as well as chemical kinetics of a biological network. Once we have these systems of equations for our particular application, they can then be stacked into vector to yield an equation of the form:

$$\dot{x} = f(x). \tag{1.8}$$

For example, the equations in (1.7) would become:

$$\dot{x} = \begin{bmatrix} \dot{a} \\ \dot{b} \\ \dot{c} \\ \dot{e} \end{bmatrix} \text{ and } f(x) = \begin{bmatrix} -k_1 ae \\ k_3 b^2 e - k_2 c \\ k_1 ae - k_3 b^2 e + k_2 c \\ -k_1 ae + k_3 b^2 e - k_2 c \end{bmatrix}$$

In this particular case $f(x)$ contains nonlinear functions. When the functions are linear the equation in (1.8) becomes:

$$\dot{x} = Ax, \tag{1.9}$$

where $A \in \mathbb{R}^{n \times n}$ is the matrix of coefficients, often referred to as the dynamics matrix, and $x \in \mathbb{R}^n$. The A matrix contains all the information about the structure of the network. When there is an external input, $u \in \mathbb{R}^m$, into the system and output, $y \in \mathbb{R}^p$, from the system, the nonlinear system is denoted:

$$\begin{aligned} \dot{x} &= f(x, u) \\ y &= g(x, u) \end{aligned} \tag{1.10}$$

The linear equivalent of (1.10) is defined as:

$$\begin{aligned} \dot{x} &= Ax + Bu \\ y &= Cx + Du \end{aligned} \tag{1.11}$$

where A is defined as in (1.9), $B \in \mathbb{R}^{n \times m}$ is called the control matrix, $C \in \mathbb{R}^{p \times n}$ is called the sensor matrix, and $D \in \mathbb{R}^{p \times m}$ is the direct term. Note that frequently systems will not have a direct term, indicating that the control signal does not influence the output directly, [21].

Many systems, including wireless computer networks and biological networks, are nonlinear, with behavior that is difficult to study. By linearizing the system in (1.10) around an equilibrium point we can apply linear systems theory to understand the behavior of the system close to this equilibrium. An equilibrium point is defined as a pair $(x_{eq}, u_{eq}) \in \mathbb{R}^n \times \mathbb{R}^k$ such that $f(x^{eq}, u^{eq}) = 0$, resulting in $\dot{x} = 0$. The local linearization around an equilibrium point is the linear time-invariant system:

$$\begin{aligned} \dot{x} &= Ax + Bu \\ \dot{y} &= Cu \end{aligned} \tag{1.12}$$

where $A = \frac{\partial f(x^{eq}, u^{eq})}{\partial x}, B = \frac{\partial f(x^{eq}, u^{eq})}{\partial u}$ and $C = \frac{\partial g(x^{eq}, u^{eq})}{\partial x}$, where f and g are the equations from (1.10), [22].

Note that for nonlinear systems, it is also possible that the system cycles through a specific trajectory continuously, rather than staying at a specific point, until perturbed. This type of phenomenon is referred to as a limit cycle. A limit cycle exists when a system has

a *nontrivial periodic solution* such that $x(t+T) = x(t), \forall t \geq 0$, also referred to as a closed curve, [23]. If we let $\mathscr{C}$ be a closed curve, and if every trajectory moves asymptotically onto $\mathscr{C}$ as $t \to \infty$, then $\mathscr{C}$ is called a stable limit cycle, shown in Figure 1.1a. If every trajectory moves asymptotically onto $\mathscr{C}$ as $t \to -\infty$, then $\mathscr{C}$ is called an unstable limit cycle, shown in Figure 1.1b, [24].

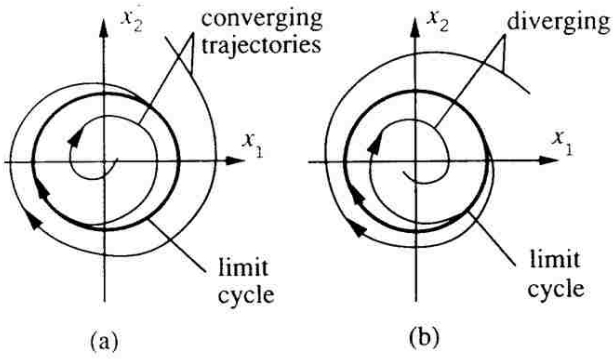

Figure 1.1: (a) Stable limit cycle, (b) Unstable limit cycle

It is possible to linearize around the limit cycle in order to apply linear systems theory, but the linearization process is beyond the scope of this thesis. It is sufficient to note that nonlinear systems can be linearized about an equilibrium, point or cycle, in order to get them into the form shown in Equation 1.11, [25]. From this point on we will ignore the nonlinear dynamics of our applications and focus on results related to linear time-invariant (LTI) systems. Once we have linearized our system about an equilibrium, its complete computational structure can then be represented graphically.

1.3.1 Complete Computational Structure

The *complete computational structure* of the system, without taking into account the concept of intricacy, [26], in (1.11) is defined as the graphical representation of the dependency among input, state, and output variables that is in direct, one-to-one correspondence with the system's state space realization, denoted $\mathscr{C}$. $\mathscr{C}$ is a weighted directed graph with vertex set $V(\mathscr{C})$ and edge set $E(\mathscr{C})$. The vertex associated with the i^{th} input is labeled u_i for

$i = 1, ..., m$ and the vertex associated with the j^{th} state is labeled j for $j = 1, ..., n$. The edge set contains an edge from node i to node j if the function associated with the label of node j depends on the variable or input labeled node i. Edges that show the dependence of a state on an input are denoted $b_{j,i}$, while the edges showing dependence among states are denoted $a_{j,i}$. Note, in some cases auxiliary variables are used to characterize intermediate computations, but since it is standard practice to eliminate auxiliary variables for simplicity, we will ignore them.

Example 2. *Consider the following system:*

$$\begin{bmatrix} \dot{x}_1 \\ \dot{x}_2 \\ \dot{x}_3 \\ \dot{x}_4 \\ \dot{x}_5 \\ \dot{x}_6 \\ \dot{x}_7 \\ \dot{x}_8 \\ \dot{x}_9 \\ \dot{x}_{10} \\ \dot{x}_{11} \\ \dot{x}_{12} \\ \dot{x}_{13} \end{bmatrix} = \begin{bmatrix} a_{1,1} & 0 & 0 & 0 & 0 & 0 & 0 & 0 & 0 & 0 & 0 & 0 & a_{1,13} \\ 0 & a_{2,2} & 0 & 0 & 0 & 0 & 0 & 0 & 0 & a_{2,10} & 0 & 0 & 0 \\ 0 & 0 & a_{3,3} & 0 & 0 & 0 & 0 & 0 & a_{3,9} & 0 & 0 & a_{3,12} & 0 \\ 0 & 0 & 0 & a_{4,4} & 0 & 0 & 0 & a_{4,8} & 0 & 0 & 0 & 0 & 0 \\ 0 & 0 & 0 & 0 & a_{5,5} & a_{5,6} & 0 & 0 & 0 & 0 & 0 & 0 & 0 \\ 0 & 0 & 0 & a_{6,4} & 0 & a_{6,6} & 0 & 0 & 0 & 0 & 0 & 0 & 0 \\ 0 & 0 & 0 & 0 & a_{7,5} & 0 & a_{7,7} & 0 & 0 & 0 & 0 & 0 & 0 \\ a_{8,1} & a_{8,2} & 0 & 0 & 0 & 0 & a_{8,7} & a_{8,8} & 0 & 0 & 0 & 0 & 0 \\ 0 & 0 & 0 & a_{9,4} & 0 & 0 & 0 & 0 & a_{9,9} & 0 & 0 & 0 & 0 \\ 0 & 0 & 0 & 0 & 0 & 0 & 0 & 0 & 0 & a_{10,10} & a_{10,11} & 0 & 0 \\ 0 & 0 & a_{11,3} & 0 & 0 & 0 & 0 & 0 & 0 & 0 & a_{11,11} & 0 & 0 \\ 0 & 0 & 0 & 0 & 0 & 0 & 0 & 0 & 0 & 0 & 0 & a_{12,12} & 0 \\ 0 & 0 & 0 & 0 & 0 & 0 & 0 & 0 & 0 & 0 & 0 & 0 & a_{13,13} \end{bmatrix} \begin{bmatrix} x_1 \\ x_2 \\ x_3 \\ x_4 \\ x_5 \\ x_6 \\ x_7 \\ x_8 \\ x_9 \\ x_{10} \\ x_{11} \\ x_{12} \\ x_{13} \end{bmatrix} + \begin{bmatrix} 0 & 0 & 0 \\ b_{2,1} & 0 & 0 \\ 0 & 0 & 0 \\ 0 & 0 & b_{4,3} \\ 0 & 0 & 0 \\ 0 & 0 & 0 \\ 0 & 0 & 0 \\ 0 & 0 & 0 \\ 0 & 0 & 0 \\ 0 & 0 & 0 \\ 0 & 0 & 0 \\ 0 & b_{12,2} & 0 \\ b_{13,1} & 0 & 0 \end{bmatrix} \begin{bmatrix} u_1 \\ u_2 \\ u_3 \end{bmatrix} \tag{1.13}$$

The complete computational structure associated with the system in Equation 1.13 is:

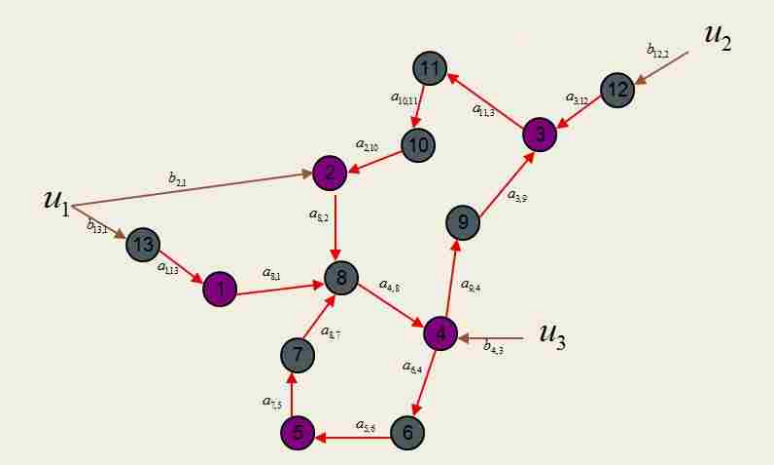

Figure 1.2: Complete Computational Structure

The complete computational structure describes both the system's structure and dynamics, but it can often be too complicated to understand the nature of the whole system

with this representation. In this case, simpler representations of the network, such as the subsystem structure or signal structure, could be more useful, [26].

1.3.2 Subsystem Structure

Subsystem structure refers to the interconnection structure of the subsystems of a given system. Given the system with realization (1.11) and associated computational structure, the *subsystem structure* is a condensation graph, a graph created by collapsing several nodes in the complete computational structure into a single node for each subsystem, $\mathscr{S}$ of $\mathscr{C}$ with vertex set $V(\mathscr{S})$ and edge set $E(\mathscr{S})$ given by:

- $V(\mathscr{S}) = \{S_1, ..., S_q\}$ are the elements of an admissible partition of $V(\mathscr{C})$, where q is the number of distinct subsystems, and
- $E(\mathscr{S})$ has an edge (S_i, S_j), labeled y_k, if $E(\mathscr{C})$ has an edge from some component of S_i to some component of S_j

We label the nodes of $V(\mathscr{S})$ with the transfer function of the associated subsystem, which we also denote S_i, and the edges of $E(\mathscr{S})$ with the associated variable from $E(\mathscr{C})$.

Example 3. *The subsystem structure of the system of the system given in Equation 1.13 with complete computational structure in Figure 1.2 is given by:*

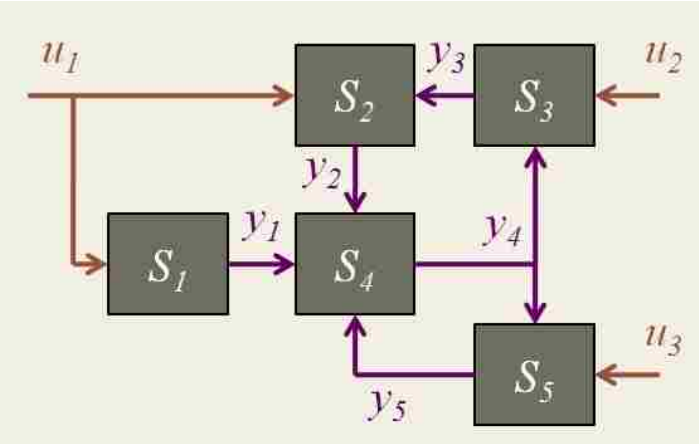

Figure 1.3: Subsystem Structure

The subsystems in Figure 1.4 are $S_1 = \{1, 13\}$, $S_2 = \{2, 10, 11\}$, $S_3 = \{3, 9, 12\}$, $S_4 = \{4, 7, 8\}$ and $S_5 = \{5, 6\}$.

1.3.3 Signal Structure

Another natural way to partially describe the structure of a system is to characterize the open-loop causal dependence among each of its manifest variables. The state space of the system is shown in Equation 1.11 and we will consider the case when $C = \begin{bmatrix} I & 0 \end{bmatrix}$. This will split the state variables into two parts: $\begin{bmatrix} x_1 \\ x_2 \end{bmatrix}$, where x_1 contains the measured states and x_2 contains the hidden states.

The full derivation for dynamical structure functions can be found in [26], but the main result is:

$$X_1 = Q(s)X_1 + P(s)U \tag{1.14}$$

where X_1 and U are the Laplacians for x_1 and u, respectively, $Q(s) = (sI - D(s))^{-1}(W(s) - D(s))$ and $P(s) = (sI - D(s))^{-1}V(s)$. Furthermore, $W(s) = \begin{bmatrix} A_{11} + A_{12}(sI - A_{22})^{-1}A_{21} \end{bmatrix}$, $V(s) = \begin{bmatrix} B_1 + A_{12}(sI - A_{22})^{-1}B_2 \end{bmatrix}$ and $D(s)$ is defined to be a diagonal matrix whose entries are the diagonal values of $W(s)$. The matrices $(Q(s), P(s))$ are called the dynamical structure functions of the system.

The *signal structure* of a system with realization (1.11) and dynamical structure function $(Q(s), P(s))$ characterized by (1.14), is a graph $\mathscr{W}$, with a vertex set $V(\mathscr{W})$ and edge set $E(\mathscr{W})$ given by:

- $V(\mathscr{W}) = \{u_1, ..., u_m, y_{11}, ..., y_{1p_1}, y_{21}, ..., y_{2p_2}\}$, each representing a manifest variable of the system, and
- $E(\mathscr{W})$ has an edge from u_i to y_{1j} or y_{1i} to y_{1j} if the associated entry in $P(s)$ or $Q(s)$ (as given in Equation (1.14)) is nonzero, respectively.

We label the nodes of $V(\mathscr{W})$ with the number of the associated variable, and the edges of $E(\mathscr{W})$ with the associated transfer function entry of $Q(s)$ or $P(s)$ from Equation (1.14).

Example 4. *The signal structure of the system in Equation 1.11 with complete computational structure in Figure 1.2 is:*

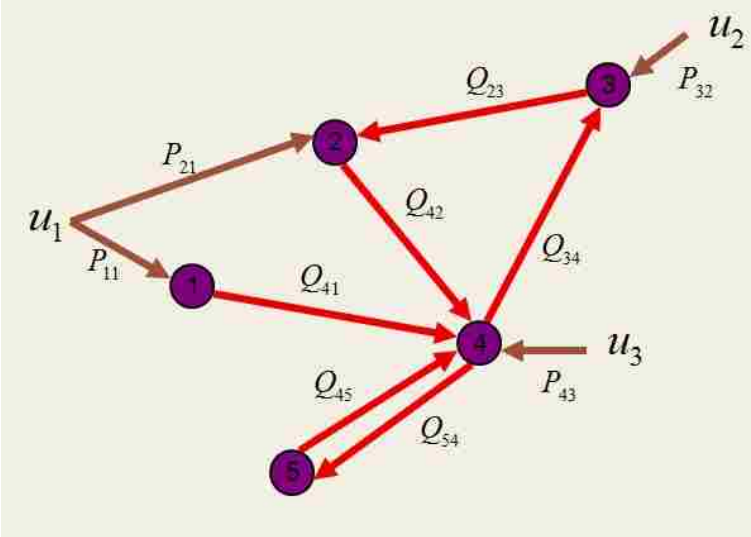

Figure 1.4: Signal Structure

With these different notions of structure defined, we can discuss how they each affect the reconstruction process.

1.3.4 Network Reconstruction

The reconstruction process begins with data, usually input-output data, from the system and attempts to determine the parameters of a model of the system. The first step, as shown in Figure 1.5, is referred to as system identification.

The purpose of system identification is to determine the mathematical model of input-output behavior of a system from data. This model is referred to as the system's transfer function, G, which represents the input-output relationship of a linear time invariant system by:

$$y = Gu \tag{1.15}$$

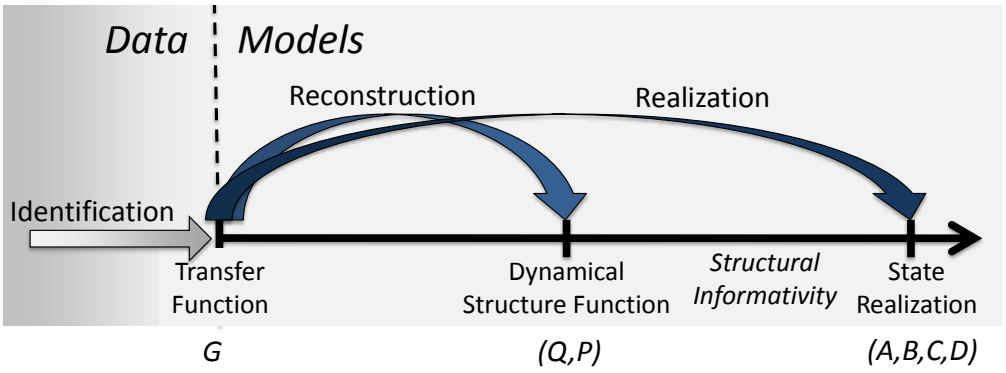

Figure 1.5: The Reconstruction Process

where $u \in \mathbb{R}^m$ is the input to a system and $y \in \mathbb{R}^p$ is the output of the system. G is a black box representation of the system, containing no information about the structure. The system identification process for determining a system's transfer function from input-output data has been well studied and there exist many methods for transfer function identification, [27].

The transition from a system's transfer function to its state space form is called realizing the system, as shown in Figure 1.5. Attempting to determine the state space realization for a system given the system's transfer function, G, is an ill-posed problem since there are many state space realizations for a single transfer function matrix. The only way to realize the system and yield the state space model is if the system has full state feedback, meaning that every node in the system is measured. Since this is not generally possible for biological networks, various assumptions are made about the system a priori before the state space realization can be determined.

Thus, reconstructing the system to a partial structure representation, so that less extra information is required, would be more desirable than attempting to realize the entire system. The process of network reconstruction from a system's transfer function to its subsystem structure, (N, S), is known to be difficult, evidenced by the lack of literature in the field. So, in order to reconstruct a biological network with weak a priori information, dynamical structure functions were developed to represent the system's signal structure.

Dynamical structure functions represent networks in terms of Q and P as defined in (1.14). The relationship between a system's dynamical structure function (Q, P) and its transfer function G is given by:

$$G = (I - Q)^{-1}P$$

In [28], sufficient conditions for reconstruction of biological networks using dynamical structure functions were shown for diagonal P. This work seeks to extend these results to determine necessary and sufficient informativity conditions as well as detailing a methodology for robust reconstruction of networks.

Chapter 2

Related Work

With the network reconstruction process detailed, it is also pertinent to understand the various network reconstruction methods that are available. Improvements in technology have led to the advent of a plethora of reconstruction algorithms that are being developed at a rate that is doubling every two years, [29]. The flood of algorithms led to the creation of the DREAM (Dialogue on Reverse Engineering Assessment and Methods) competition at MIT, whose purpose it is to assess the performance of network reconstruction algorithms. Available inference techniques include correlation-based methods (discussed in Section 2.1), Bayesian network predictions (discussed in Section 2.2), and methods based on dynamical models (discussed in Section 2.3), [29]. After looking at the reconstruction methods, we discuss reconstruction as is relates specifically to the applications of biological systems in Section 2.4 and wireless networks in Section 2.5.

2.1 Correlation Methods

The first attempts at network reconstruction came by way of correlation studies, which was invented over a century ago by Francis Galton who stated that correlation between two variables measured the extent to which the variables were governed by "common causes," [30]. Modern correlation methods attempt to determine correlations between species through perturbation experiments, [31] and [32]. However, Karl Pearson and his assistant G. Udny Yule, whose works came roughly a decade after Galton and who were instrumental in the

development of correlation analysis, discussed a limitation of correlation analysis, namely "misleading," or "spurious" correlations: which refers to variables A and B that are not directly causally related, but are both effects of C, [33]. This reveals an inherent problem in the application of correlation studies to network inference. While certain species may appear correlated, that does not necessarily guarantee that connections exist between them. Moreover, although there have been efforts to remove spurious connections after performing the correlation analysis, it may not be possible to remove all the spurious edges in order to determine the correct network, [34].

2.2 Bayesian Networks

In order to overcome the weakness of correlation methods, a popular technique for reconstruction has been to infer the probability of connections between species using Bayesian networks. Bayesian networks are graphical models in which each node represents a random variable and each edge represents the probabilistic dependence among the corresponding random variables. The main problem with applying Bayesian networks to the network reconstruction of biochemical networks is that their structure corresponds to a directed acyclic graph (DAG), while cycles tend to appear frequently in biochemical and wireless networks, [35].

Due to this limitation, some researchers in biology have focused on network reconstruction in areas of biology where DAGs are common, such as pedigree analysis, where the distribution of a genotype depends on the genotype of its biological parents, or phylogenetic models, which studies the probability of different evolutionary sequences occurring in species, [36]. Wireless network researchers also tend towards problems where DAGs are prevalent, such as the analysis of cognitive networks [37] or indoor positioning systems for location estimation of wireless devices [38].

Another approach has been to use dynamic Bayesian networks, which are able to handle cyclic networks by using time series information, [39]. However, inference using dynamic Bayesian networks is slow, even when the network is sparse, since the minimum

size of the posterior distribution for any arbitrary time slice is generally exponential in the number of variables that have parents in the previous slice, [40].

Many inference algorithms suffer from issues with time complexity, even network reconstruction with DSF contains a combinatoric search when noise is present in the system and robust reconstruction is necessary, although it has been shown that under certain conditions this time complexity can be reduced to polynomial time, [41]. There have been attempts by several researchers to rectify this issue, such as the Reverse Engineering Algorithm developed in [42] which utilizes dynamical models and was developed specifically for the reconstruction of large networks, but even that still has problems with computational complexity.

2.3 Dynamic Models

Dynamic models are defined as models that take the following as input: (1) interactions and regulatory relationships between components, (2) how the strength of the interactions depends on the state of the interacting components and (3) initial state of each component in the system, and produce as output the time evolution of the state of the system, [43]. Since the description of a dynamic model is so broad, they are often modeled with varying degrees of detail and model flexibility. The highest level of detail are found in differential equations and stochastic models, which contain the most information about the system computationally demanding when attempting to reconstruct a network and often require accurate measurements. At the other end of the spectrum lies promotion-inhibition networks, which are incredibly simple in that they assume a chemical species is either on or off and have the advantage of being easy to interpret and robust, [44].

The state space model, as outlined in Section 1.3, falls into the category of being an extremely detailed dynamic model. As noted in Section 1.3.4, the realization of the state space model from a system's transfer function is ill-posed. In order to overcome this, researchers attempted to find the state space that fit the assumption that the sparsest system

was the actual system, [45]. However, this is a poor assumption because "parsimony is not the correct criterion for selection of biological regulatory networks since the evolution selects the networks that are robust and redundant rather than parsimonious," [46].

Another common assumption is that the structure of a system is known a priori in a very strong sense, such as an entire partition of the overall state space is assumed to be known, [47], [48]. However, while "assuming knowledge of such a partition may be reasonable in some cases, especially when considering engineered systems... in other situations, however, assuming a priori knowledge of a partition over the entire state space of the complex system could be unreasonable. For example, when modeling a chemical reaction network of a biological system," [49]. Therefore, a more suitable network reconstruction technique would require less a priori information.

A look at the other end of the spectrum are simplified models such as a promotion-inhibition model in biological networks, [50]. While simple representations have their benefits, their dynamics are often too strict. In the promotion-inhibition example, not every species in a network can be measured, the connections between certain species may be promoting in some instances and inhibiting in other instances, depending on the hidden variables in the system. A more accurate model of the system would not compromise these dynamics.

The benefit of utilizing dynamical structure functions is that it requires only weak a priori information when compared to the realization process, [49], and it contains more information about the dynamics of the system than a simple promotion-inhibition graph. Although current results only hold for a diagonal P, this thesis presents necessary and sufficient conditions for network reconstruction even without assuming target specificity of controlled inputs.

2.4 Direction of Research in Systems Biology

Having reviewed the reconstruction process in general, we now take a quick look at how systems biology has been evolving in recent years, leading to a renewed interest in improvements

in the field, such as that of network reconstruction. In the preface to [51] the editors note several reasons for increased interest in systems biology recently as well as the direction of research in the area. Firstly, a greater understanding of molecular mechanisms has led to an increased focus on cell physiology. Secondly, experimental techniques have improved, allowing for new opportunities for investigating cellular behavior, including new "high-throughput" technologies allowing for the analysis of system-wide behavior.

According to [52], computational modeling and analysis have now become useful in providing useful biological insights and predictions for well understood such as the bifurcation analysis of the cell cycle, metabolic analysis or comparative studies of robustness of biological oscillation circuits. This is not only because of improvements in biological experiments and the understanding of cell structure, but also because of advances in software and computational power has enabled the creation and analysis of reasonably realistic yet intricate biological models.

2.5 Interference Maps for Wireless Networks

Just as improved technology has helped in systems biology, it has been imperative in the development of wireless network technology. As noted in [14] wireless networking is increasingly being used to deploy enterprise LANs and multi-hop mesh networks, especially in rural areas. One of the difficulties that arises in deploying and maintaining a wireless network is dealing with contention and interference, which can cause performance degradation, [53–55].

One way to manage contention and interference in a wireless network is to develop an interference map of the network [11, 56]. Using the interference map a network manager can then rearrange nodes in order to reduction contention and interference, [57, 58].

There are two main approaches for developing an interference map of a wireless network. The first approach uses controlled offline experiments, measuring the contention between two nodes at a time in the network, [11, 56, 59]. Using broadcast measurements,

this approach only requires experiments on the order of $O(n^2)$ [11, 56]. One attempt of this approach reduced the complexity to $O(n)$, but ignored remote interferers, [59], although it has been shown that remote interferers are the main source of interference in a wireless network, [11].

The second approach for developing an interference map uses online, passive measurements of the network to determine contention and interference relationships. Some attempts of this approach have used packet sniffing, [60, 61]. However, one disadvantage of using packet sniffing is that nodes must be synchronized. Another attempt at this approach collected traffic from existing network flows, then used regression analysis to infer relationships among them [62]. However, this technique is unable to distinguish between direct and indirect relationships. Another online method is known as microprobing, where two nodes are synchronized to simultaneously send a small probe packet in order to determine the relationship between them, [63].

This thesis presents a method for determining a type of interference map of a wireless network, in this case the open-loop causal dependencies between sending rates on links, i.e. how the sending rate of one link affects the rates of other links. The benefit of the method presented is that we can create the map while the network is online and we are able to detect the presence of transitory unidentified nodes and devices which are not part of the managed structure.

Chapter 3

Foundational Material

Before delving into the new results, we begin by outlining the evolution of the network reconstruction process associated with Dynamical Structure Functions. First, we note that the dynamical structure function (Q, P) is not uniquely specified for a given transfer function G without a priori information. Thus, we require informativity conditions that state exactly what information about the network is required so that the pair (Q, P) is uniquely specified. In [28] sufficient informativity conditions were given for reconstruction when no noise is present within the system, discussed in Section 3.1.

Having shown that reconstruction was possible under certain conditions without noise present in the system, [1] presents two robust reconstruction techniques allowing for reconstruction when noise is present in the system. The first reconstruction technique calculates Q and P from G while the other reconstructs directly from input-output data. In Sections 3.2 and 3.3 we outline each method, as well as the advantages and disadvantages of each.

Finally, in Section 3.4 we highlight an important aspect of the robust reconstruction process: using an information criterion to penalize extra connections. This is useful in the reconstruction process since the robust reconstruction methods tend to favor networks that contain more links, even when the actual network is sparse.

3.1 Sufficient Informativity Conditions for Network Reconstruction

Sufficient informativity conditions for network reconstruction with dynamical structure functions was outlined in [28], first noting that reconstruction without a priori information about the system was not possible in the following theorem:

Theorem 1. *Given any $p \times m$ transfer function G, with $p > 1$ and no other information about the system, dynamical and Boolean reconstruction. Moreover, for any internal structure Q, there is a dynamical structure function (Q, P) that is consistent with G.*

The sufficient conditions for reconstruction, noting what a priori information allowed for reconstruction, were then outlined in the following theorem:

Theorem 2. *Given a $p \times m$ transfer function G, dynamical structure reconstruction is possible from partial structure information if $p-1$ elements in each column of $\begin{bmatrix} Q & P \end{bmatrix}'$ are known that uniquely specify the component of (Q, P) in the nullspace of $\begin{bmatrix} G' & I \end{bmatrix}$.*

Using these sufficient conditions, the authors of [28] noted that a diagonal P is a sufficient condition for reconstruction in the following corollary:

Corollary 1. *If $m = p$, G is full rank, and there is no information about the internal structure of the system Q, then the dynamical structure can be reconstructed if each input directly controls a measured state independently (i.e., without loss of generality, the inputs can be numbered such that P is diagonal). Moreover, $H = G^{-1}$ characterizes the dynamical structure as follows:*

$$Q_{ij} = -\frac{H_{ij}}{H_{ii}} \text{ and } P_{ii} = \frac{1}{H_{ii}}.$$

A system with diagonal P, as this corollary notes, is one one where each measured state can be independently controlled. This sufficient condition for reconstruction severely restricted the systems that could be reconstructed. This thesis extends these results to show

exactly what information is necessary and sufficient for reconstruction, even when P is not diagonal. Note that this does not mean that we can reconstruct every network, we simply determine under what conditions a system can be reconstructed without the restriction that P is diagonal.

3.2 Robust Reconstruction from G

While we can solve for Q and P exactly from G under the conditions in Corollary 1, finding Q and P exactly is almost impossible for real or simulated systems when noise is present in the system. So, in [1], it was shown that if noise is present, one can determine the dynamical structure function from a stable transfer function G using a robust reconstruction method when P was diagonal.

First, the transfer function is identified from noisy time-series data using standard system identification tools, [64]. Since noise is present in the system, reconstructing perfectly from G is no longer possible using Corollary 1 since the noise would lead to a dynamical structure function in which the internal structure function Q would appear to be fully connected, even if it wasn't. In order to overcome this, the *distance* from G to all possible boolean structures (of which there are 2^{p^2-p} of them) is quantified. Structures with small distances are candidates for the correct structure of the network, while those that have large distances associated with them are unlikely to be the correct structure, a thresholding process is used to determine what constitutes "small" and what constitutes "large".

There are many ways to model input-output data with noise and nonlinearities, in [1] a feedback uncertainty on the output was considered as it yielded a convex optimization problem, [65]. Using this framework, the true system is given by $(I+\Delta)^{-1}G$, where Δ represents unmodelled dynamics, such as noise and nonlinearities. Given the true system, the distance from data to a particular Boolean structure is chosen by minimizing $||\Delta||$ such that Q obtained from $(I+\Delta)^{-1}G = (I-Q)^{-1}P$ has the desired Boolean structure. Solving for Δ, we can rewrite the above equation as $\Delta = GP^{-1}(I-Q) - I$. Letting $X = P^{-1}(I-Q)$,

the Boolean structure constraint on Q can be reformulated on X, i.e., non-diagonal zero elements in X correspond to those in Q since $X_{ij} = P_{ii}^{-1} Q_{ij}$ for $i \neq j$.

Now ordering all Boolean structures from 1 to 2^{p^2-p}, and defining a set χ_k containing transfer function matrices that satisfy the following conditions: (i) for $i \neq j$, $X_{ij}(s) = 0$ if for the considered k^{th} Boolean structure $Q_{ij}(s) = 0$; all other $X_{ij}(s)$ are free variables; (ii) when $i = j$, $X_{ii}(s)$ is a free variable. The distance from G to a particular Boolean structure can be written as $\alpha_k = \inf_{X \in \chi_k} ||GX - I||^2$, which is a convex minimization problem with a careful choice of norm. Next, we show that this problem can be cast as a least squares optimization problem. If we use the norm defined by $||\Delta||^2 =$ sum of all $||\Delta_{ij}||_2^2$, where $||\cdot||_2$ stands as the $\mathcal{L}_2$-norm over $s = j\omega$, then using the projection theorem [66] the problem reduces to:

$$\alpha_k = \sum_i ||A_i (A_i^* A_i)^{-1} A_i^* e_i - e_i||_2^2$$

where A_i is obtained by deleting the j^{th} columns of G when the corresponding elements $X_i[j]$ are 0 for all j, and $(\cdot)^*$ denotes transpose conjugate.

3.3 Robust Reconstruction from Data

Although the previous method for robust reconstruction works well, information can be lost when determining a system's transfer function G from data and then reconstructing to find the dynamical structure function (Q, P) from G. Thus, another method was also proposed in [1] that allows for the reconstruction of the dynamical structure function (Q, P) directly from data. Rather than feedback uncertainty, this method considers additive uncertainty on the output, i.e., $Y = G_\Delta(U + \Delta)$. In this case, the distance is how much the input much be changed in order for the reconstructed system to fit a particular Boolean structure. Since $G_\Delta = (I - Q)^{-1} P = X^{-1}$, the equality $Y = G_\Delta(U + \Delta)$ can be written as

$$\Delta = XY - U,$$

where $X \in \chi_k$ for some particular Boolean network k. Recall that structural constraints in Q can be imposed directly on X from the equality $X = P^{-1}(I - Q)$. Then, using system identification tools for non-causal auto-regression models under the structural constraints one can identify X (which might be non-causal). In this case the distance is defined as the maximum likelihood of the estimation problem.

3.4 Penalizing Connections using an Information Criterion

While the two robust reconstruction methods are theoretically sound, there is an inherent flaw associated with both of them. Namely, that there are several candidate structures with distances smaller than the true structure of the system. For example, since the fully connected network has extra degrees of freedom its corresponding distance α_k is the smallest of all. This is similar to the problem of noisy data over-fitting encountered in system identification when attempting to determine the correct transfer function of a system, where a higher order transfer function yields a better fit. The typical approach in system identification to pick a more correct transfer function is to penalize higher dimensions and the analogy in the network reconstruction case is to penalize extra network connections, [1].

Consider the case that the true network has l non-existent connections, i.e. l off-diagonal elements in Q are zero, then there are $2^l - 1$ different Boolean networks that have a smaller or equal distance due to the extra degrees of freedom provided by the additional connections for those network structures. In the case when noise is present, the true network structure will typically have a distance similar to those other l structures. The question of how to find the true network from among these candidate structures then arises. With repeated experiments, small enough noise (i.e., large enough signal-to-noise ratio) and negligible nonlinearities, the distances associated with those l networks are comparable, and they are usually much smaller than those of the other networks.

Now, in order to determine the correct network structure, one must find a balance between network complexity and data fitness by taking into account the associated distance

along with penalizing extra connections. There are several ways to do this, one of which is Akaikes Information Criterion (AIC) [67], or some of its variants such as AICc, which is AIC with a second correction for small sample sizes, and the Bayesian Information Criterion (BIC) [68].

AIC is tool for model selection, so, given a data set, several competing models may be ranked according to their AIC value, with the one having the lowest AIC being the best model. The AIC value for a particular Boolean network B_k is defined in [1] as

$$AIC_k = 2L_k + 2ln(\alpha_k),$$

where L_k is the number of (non-zero) connections in the Boolean network B_k and α_k is the optimal distance for this Boolean network.

Chapter 4

Necessary and Sufficient Informativity Conditions

As noted in Section 3.1, previous results only provided sufficient informativity conditions for the reconstruction of a network. The first contribution of this thesis are conditions that are both necessary and sufficient for network reconstruction using dynamical structure functions, found in Section 4.1. Having established the necessary and sufficient informativity conditions, in Section 4.2 several examples of the reconstruction of dynamical structure functions utilizing these conditions are detailed.

4.1 Necessary and Sufficient Conditions for Network Reconstruction

As in Section 3.2, we will assume that the system's transfer function has been successfully identified from data using standard system identification tools, [64]. Thus, we will focus on necessary and sufficient informativity conditions that detail exactly what information is needed a priori to ensure that for a given transfer function G the corresponding dynamical structure function (Q, P) is uniquely specified. To accomplish this, we will construct a mapping from the elements of the dynamical structure function to the associated transfer function and establish conditions to ensure this mapping is injective.

To facilitate the discussion, we introduce the following notation. Let $A \in \mathbb{C}^{n\times m}$ and $B \in \mathbb{C}^{k\times l}$. Then:

- blckdiag(A, B) is the block diagonal matrix given by

$$\begin{bmatrix} A & 0 \\ 0 & B \end{bmatrix},$$

- a_i is the i^{th} column of matrix A,
- A_{-i} is the matrix A without it's i^{th} column,
- a_{ij} is the $(i,\, j)^{th}$ entry of matrix A,
- A' is the conjugate transpose of matrix A,
- $\mathcal{R}(A)$ is the range of A,
- $\overrightarrow{a}$ is the vector stack of the columns of A, given by

$$\begin{bmatrix} a_1 \\ a_2 \\ \vdots \\ a_m \end{bmatrix}$$

- and $\overleftarrow{a}$ is the vector stack of the columns of A'.

The construction of a map from elements of the dynamical structure function to the associated transfer function begins by rearranging Equation (4.1) from the following Lemma, which was proven in [69]:

Lemma 1. *The transfer function, G, of the system* $\begin{bmatrix} \dot{y} \\ \dot{x} \end{bmatrix} = \begin{bmatrix} A_{11} & A_{12} \\ A_{21} & A_{22} \end{bmatrix} \begin{bmatrix} y \\ x \end{bmatrix} + \begin{bmatrix} B_1 \\ B_2 \end{bmatrix} u,\ y = \begin{bmatrix} I & 0 \end{bmatrix} \begin{bmatrix} y \\ x \end{bmatrix}$, *is related to its dynamical structure, (Q, P), by*

$$G = (I - Q)^{-1} P \tag{4.1}$$

to get:

$$\begin{bmatrix} I & G' \end{bmatrix} \begin{bmatrix} P' \\ Q' \end{bmatrix} = G' \tag{4.2}$$

Noting that

$$AX = B \iff \text{blckdiag(A, ..., A)}\vec{x} = \vec{b}$$

and defining $X = \begin{bmatrix} P' & Q' \end{bmatrix}'$ then allows us to rewrite Equation (4.2) as

$$\begin{bmatrix} I & \text{blckdiag}(G', ..., G') \end{bmatrix} \overleftarrow{x} = \overleftarrow{g}\,. \tag{4.3}$$

Further noting that since the diagonal elements of Q are identically zero and the dimensions of P, Q, and G are $p \times m$, $p \times p$, and $p \times m$ respectively, then exactly p elements of $\overleftarrow{x}$ are always zero. Abusing notation, we can then redefine $\overleftarrow{x}$ to remove these zero elements, reducing Equation (4.3) to the following:

$$\begin{bmatrix} I & \text{blckdiag}(G'_{-1}, G'_{-2}, ..., G'_{-p}) \end{bmatrix} \overleftarrow{x} = \overleftarrow{g}\,. \tag{4.4}$$

Equation (4.4) reveals the mapping from elements of the dynamical structure function, contained in $\overleftarrow{x}$, to its associated transfer function, represented by $\overleftarrow{g}$. The mapping is clearly a linear transformation represented by the matrix operator $\begin{bmatrix} I & \text{blckdiag}(G'_{-1}, G'_{-2}, ..., G'_{-p}) \end{bmatrix}$. This matrix has dimensions $(pm) \times (pm + p^2 - p)$, and thus the transformation is certainly not injective. This is why not even the Boolean structure of a system's dynamical structure function can be identified – even from perfect information about the system's transfer function – without additional a priori structural information.

Identifiability conditions will thus be established by determining which elements of $\overleftarrow{x}$ must be known a priori in order to reduce the corresponding transformation to an injective

map. To accomplish this, consider the $(pm + p^2 - p) \times k$ transformation T such that

$$\overleftarrow{x} = Tz \tag{4.5}$$

where z is an arbitrary vector of k transfer functions.

Lemma 2. *Let*

$$M = LT, \tag{4.6}$$

where $L = \begin{bmatrix} I & \text{blckdiag}(G'_{-1}, G'_{-2}, ..., G'_{-p}) \end{bmatrix}$ *and* T *is a* $(pm + p^2 - p) \times k$ *matrix operator as in Equation (4.5). Then* M *is injective if and only if rank*$(M) = k$.

Proof. This stems from the fact that M is a $pm \times k$ matrix, and M is injective iff it has full column rank, meaning rank$(M) = k$. □

Theorem 3. (Identifiability Conditions) *Given a system characterized by the transfer function* G*, its dynamical structure function* (Q, P) *can be identified if and only if*

1. M*, defined as in Equation (4.6), is injective, and*
2. $\overleftarrow{g} \in \mathcal{R}(M)$.

Proof. The proof follows immediately from the observation that M is the mapping from unidentified model parameters to the system transfer function, i.e. $Mz = \overleftarrow{g}$. Under these conditions one can clearly solve for z given G and then construct the dynamical structure function. □

4.2 Necessary and Sufficient Informativity Conditions Examples

We will now illustrate this reconstruction result on some simple examples.

Example 5. *Consider a system with square transfer function given by*

$$G = \begin{bmatrix} G_{11} & G_{12} & ... & G_{1p} \\ G_{21} & G_{22} & & G_{2p} \\ \vdots & & \ddots & \vdots \\ G_{p1} & G_{p2} & ... & G_{pp} \end{bmatrix}.$$

Previous work has shown that if G is full rank and it is known, a priori, that the control structure P is diagonal that reconstruction is possible [69]. Here we validate that claim by demonstrating that the associated T matrix becomes:

$$\begin{bmatrix} P_{11} \\ P_{12} \\ \vdots \\ P_{21} \\ P_{22} \\ \vdots \\ P_{pp} \\ Q_{12} \\ \vdots \\ Qp(p-1) \end{bmatrix} = \begin{bmatrix} 1 & 0 & ... & 0 & 0 \\ 0 & 0 & ... & 0 & 0 \\ \vdots & \vdots & \ddots & & \vdots \\ 0 & 0 & ... & 0 & 0 \\ 0 & 1 & ... & 0 & 0 \\ \vdots & \ddots & & \ddots & \vdots \\ 0 & ... & 1 & ... & 0 \\ 0 & ... & 0 & 1 & 0 \\ \vdots & \ddots & \vdots & \ddots & \vdots \\ 0 & ... & 0 & 0 & 1 \end{bmatrix} \begin{bmatrix} P_{11} \\ P_{22} \\ \vdots \\ P_{pp} \\ Q_{12} \\ \vdots \\ Q_{p(p-1)} \end{bmatrix}$$

yielding the operator $M = LT$ as:

$$M = \begin{bmatrix} e_1 & 0 & 0 & G'_{-1} & ... & 0 \\ 0 & \ddots & 0 & 0 & \ddots & 0 \\ 0 & ... & e_p & 0 & ... & G'_{-p} \end{bmatrix}$$

where e_i is a zero vector with 1 in the i^{th} position. Note that M is a square matrix with dimensions $p^2 \times p^2$ and will be invertible provided G is full rank, thus enabling reconstruction.

Example 6. *Given the following transfer function of a system:*

$$G = \begin{bmatrix} \frac{s+2}{s^2+3s+1} & -\frac{s^2+3s+3}{(s+2)(s^2+3s+1)} \\ \frac{s+2}{(s+1)(s^2+3s+1)} & \frac{s^2+s-1}{(s+1)(s^2+3s+1)} \end{bmatrix}$$

We attempt to find the dynamical structure functions (Q, P) of the system:

$$Q = \begin{bmatrix} 0 & Q_{12} \\ Q_{21} & 0 \end{bmatrix} \text{ and } P = \begin{bmatrix} P_{11} & P_{12} \\ P_{21} & P_{22} \end{bmatrix}$$

yielding the vector of unknowns $\vec{x} = \begin{bmatrix} P_{11} & P_{12} & P_{21} & P_{22} & Q_{12} & Q_{21} \end{bmatrix}'$. This gives us the system of equations of the form $L\vec{x} = \vec{b}$:

$$\begin{bmatrix} 1 & 0 & 0 & 0 & \frac{s+2}{(s+1)(s^2+3s+1)} & 0 \\ 0 & 1 & 0 & 0 & \frac{s^2+s-1}{(s+1)(s^2+3s+1)} & 0 \\ 0 & 0 & 1 & 0 & 0 & \frac{s+2}{s^2+3s+1} \\ 0 & 0 & 0 & 1 & 0 & -\frac{s^2+3s+3}{(s+2)(s^2+3s+1)} \end{bmatrix} \begin{bmatrix} P_{11} \\ P_{12} \\ P_{21} \\ P_{22} \\ Q_{12} \\ Q_{21} \end{bmatrix} = \begin{bmatrix} \frac{s+2}{s^2+3s+1} \\ -\frac{s^2+3s+3}{(s+2)(s^2+3s+1)} \\ \frac{s+2}{(s+1)(s^2+3s+1)} \\ \frac{s^2+s-1}{(s+1)(s^2+3s+1)} \end{bmatrix}$$

Without additional information a priori structural information, we can not reconstruct. Suppose, however, that we know a priori that P takes the form:

$$P = \begin{bmatrix} P_{11} & -P_{11} \\ 0 & P_{22} \end{bmatrix}$$

Note that this non-diagonal P fails to meet the previous conditions for reconstruction [69], [1]. Nevertheless, the vector of unknowns $\vec{x}$ can then be decomposed into the form $T\vec{z}$ as follows:

$$T = \begin{bmatrix} 1 & 0 & 0 & 0 \\ -1 & 0 & 0 & 0 \\ 0 & 0 & 0 & 0 \\ 0 & 1 & 0 & 0 \\ 0 & 0 & 1 & 0 \\ 0 & 0 & 0 & 1 \end{bmatrix} \quad and \ \vec{z} = \begin{bmatrix} P_{11} & P_{22} & Q_{12} & Q_{21} \end{bmatrix}'$$

Replacing $\vec{x}$ with $T\vec{z}$ above yields the system of equations of the form $M\vec{z} = \vec{b}$, where $M = LT$:

$$\begin{bmatrix} 1 & 0 & \frac{s+2}{(s+1)(s^2+3s+1)} & 0 \\ -1 & 0 & \frac{s^2+s-1}{(s+1)(s^2+3s+1)} & 0 \\ 0 & 0 & 0 & \frac{s+2}{s^2+3s+1} \\ 0 & 1 & 0 & -\frac{s^2+3s+3}{(s+2)(s^2+3s+1)} \end{bmatrix} \begin{bmatrix} P_{11} \\ P_{22} \\ Q_{12} \\ Q_{21} \end{bmatrix} = \begin{bmatrix} \frac{s+2}{s^2+3s+1} \\ -\frac{s^2+3s+3}{(s+2)(s^2+3s+1)} \\ \frac{s+2}{(s+1)(s^2+3s+1)} \\ \frac{s^2+s-1}{(s+1)(s^2+3s+1)} \end{bmatrix}$$

In this case M is full rank, from Theorem 3 we know that the system is reconstructible. By solving for $\vec{z} = (M)^{-1}\vec{b}$ we get the DSF to be:

$$Q = \begin{bmatrix} 0 & \frac{1}{s+2} \\ \frac{1}{s+1} & 0 \end{bmatrix} \quad and \ P = \begin{bmatrix} \frac{1}{s+1} & -\frac{1}{s+1} \\ 0 & \frac{1}{s+2} \end{bmatrix}$$

The signal structure of the system is shown in Figure 4.1

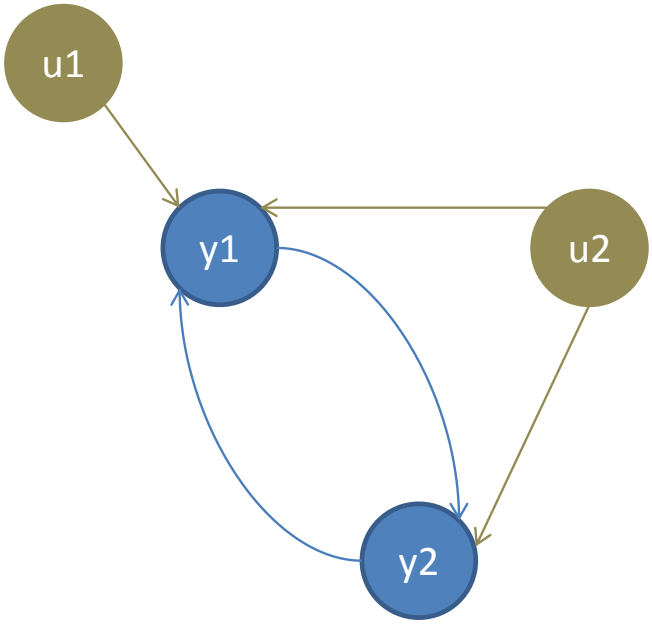

Figure 4.1: Simple Two-Node Network with Non-Diagonal P

Chapter 5

Robust Network Reconstruction

Now that we have shown that it is possible to reconstruct a system when P is not diagonal, we need new results to show how to reconstruct a system with non-diagonal P when noise is present in the system. First, we define the robust reconstruction problem in Section 5.1, which prepares us to develop a robust reconstruction algorithm for solving the problem in Section 5.2. Given a robust reconstruction algorithm, in Section 5.3 we conclude with examples of robust reconstruction for both diagonal and non-diagonal P.

5.1 Robust Reconstruction Problem

We begin by considering an additive uncertainty on the control structure P, as seen in Figure 5.1. Note that additive uncertainty over Q or both Q and P would be more interesting to consider, but since they do not appear to produce convex minimization problems we are still investigating their properties. Any results involving them will be the product of future work.

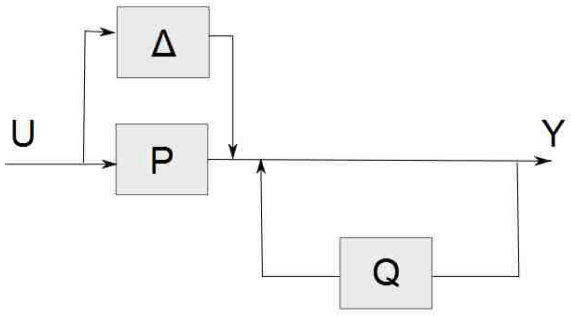

Figure 5.1: Additive uncertainty on P

The relationship we get from the block diagram in Figure 5.1 is $Y = (I-Q)^{-1}(P+\Delta)U$, where Δ represents noise and nonlinearities. Multiplying both sides by $I-Q$ we get $Y-QY = (P+\Delta)U$. Then, if we solve for ΔU, we get $\Delta U = Y - QY - PU$. This result is equivalent to $\Delta U = Y - \begin{bmatrix} Q & P \end{bmatrix} \begin{bmatrix} Y \\ U \end{bmatrix}$. Since U is a diagonal matrix, $||\Delta U|| = ||c\Delta I|| = ||c\Delta|| = |c|||\Delta||$, where $c \neq 0$ is the amount each input is perturbed. Thus, we note that minimizing $||\Delta U||$ is equivalent to minimizing $||\Delta||$, so to minimize the noise on the system, we minimize the norm:

$$\alpha = ||Y - \begin{bmatrix} Q & P \end{bmatrix} \begin{bmatrix} Y \\ U \end{bmatrix} ||$$

Stacking the unknowns from Q and P into a vector d, this can be written as $w - Md$, where w is the matrix Y stacked into a vector row by row and

$$M = \begin{bmatrix} y_2 & ... & y_n & 0 & ... & ... & 0 & u_1 & ... & u_n & 0 & ... & ... & 0 \\ 0 & ... & 0 & \ddots & 0 & ... & 0 & 0 & ... & 0 & \ddots & 0 & ... & 0 \\ 0 & ... & ... & 0 & y_1 & ... & y_{n-1} & 0 & ... & ... & 0 & u_1 & ... & u_n \end{bmatrix} \tag{5.1}$$

where y_i and u_i are the i^{th} columns of Y^T and U^T, respectively.

Therefore, we have reorganized the problem so that the norm we minimize is now $||w - Md||$, which can be solved using least squares. Note, when the system has measurement or sensor noise, both w and M will contain noise (since elements of Y are contained in both w and M). The problem then becomes the minimization of:

$$\alpha = ||(w + e_1) - (M + e_2)d|| \tag{5.2}$$

where e_1 and e_2 represent noise in the system. This new representation of the problem can then be solved using total least squares.

5.2 Robust Reconstruction Algorithm

The first step of implementation, given the input u and output y is to determine the z-transform of each to yield $Y(z)$ and $U(z)$. We do this using the finite z-transform, which is defined as:

$$X(z) = \sum_{k=0}^{N} x[k]z^{-k}$$

Now that we have $Y(z)$ and $U(z)$, we can create $M(z)$ as defined in Equation 5.1.

Next, we find every possible Boolean structure for the unknowns of Q and P, that fit the a priori information given. For each structure we do the following:

1. Use the a priori information combined with information about the current Boolean structure to restructure M. To do this, we create the matrix T defined in Equation (4.5). Then, the matrix MT incorporates the a priori information about the network. We then remove the columns of MT that correspond to the current Boolean structure.
2. For a large number of points on the unit circle, calculate α as given in 5.2, using total least squares (discussed in Section 5.2.1). Note, in theory total least squares would appear to yield better results, but in practice least squares works well. Thus, for the current Boolean structure, there will be a large number of α values associated with each point from the unit circle from which it was calculated.
3. Return the largest α value for the current Boolean structure.

Given an α for each boolean structure, we then use an information criterion to penalize connections (discussed in Section 5.2.2). The boolean structure with the smallest information criterion value should be the correct structure of the network.

5.2.1 Total Least Squares

The linear approximation problem $AX \approx B$, where $A \in \mathbb{R}^{m\times n}$, $X \in \mathbb{R}^{n\times d}$, $B \in \mathbb{R}^{m\times d}$, specified by

$$\min_{X,E,G} |||[\ G \mid E\ ]|||_F \text{ subject to } (A+E)X = B+G$$

is called the total least squares (TLS) problem with the TLS solution $X_{TLS} \equiv X$ and the correction matrix $[\ G \mid E\ ]$, with $G \in \mathbb{R}^{m\times d}$, $E \in \mathbb{R}^{m\times n}$.

Total Least Squares Solution

The solution to the Total Least Squares problem, as detailed in [70], is as follows: let $U\Sigma V^T$ be the SVD of the matrix $[\ B \mid A\ ]$, where $U^{-1} = U^T$, $V^{-1} = V^T$, $\Sigma = diag(\sigma_1, ..., \sigma_s, 0)$, $s \equiv rank([B|A])$ with the partitioning given by $\Sigma = \left[\Sigma_1^{(\Delta)}\ \Sigma_2^{(\Delta)}\right]$, where $\Sigma_1^{(\Delta)} \in \mathbb{R}^{m\times(n-\Delta)}$, $\Sigma_2^{(\Delta)} \in \mathbb{R}^{m\times(d+\Delta)}$, and $V = \begin{bmatrix} V_{11}^{(\Delta)} & V_{12}^{(\Delta)} \\ V_{21}^{(\Delta)} & V_{22}^{(\Delta)} \end{bmatrix}$ where $V_{11}^{(\Delta)} \in \mathbb{R}^{d\times(n-\Delta)}$, $V_{12}^{(\Delta)} \in \mathbb{R}^{d\times(d+\Delta)}$, $V_{21}^{(\Delta)} \in \mathbb{R}^{n\times(n-\Delta)}$, $V_{22}^{(\Delta)} \in \mathbb{R}^{n\times(d+\Delta)}$.

Furthermore, $\Delta \equiv \kappa$, $0 \le \kappa \le n$, where κ is the smallest integer such that:

1. the submatrix $V_{12}^{(\kappa)}$ is full row rank, and
2. either $\sigma_{n-\kappa} > \sigma_{n-\kappa+1}$, or $\kappa = n$.

Then $X^{(\kappa)} = -V_{22}^{(\kappa)} V_{12}^{(\kappa)\dagger}$ is the solution of the system $(A+E)X = B+G$, where $\dagger$ denotes the Moore-Penrose pseudoinverse of a matrix.

Total Least Squares Algorithm

The algorithm for solving the Total Least Squares, using the aforementioned solution, is given in [70] as the following:

00: Set $j = 0$
01: If $rank(V_{12}^{(j)}) = d$ and $j = n$, then goto line 05 02: If $rank(V_{12}^{(j)}) = d$ and $\sigma_{n-j} > \sigma_{n-j+1}$, then goto line 05 03: Set $j = j + 1$ 04: Goto line 01
05: Set $\kappa = j$ 06: Compute $X^{(\kappa)} = -V_{22}^{(\kappa)} V_{12}^{(\kappa)\dagger}$ 07: Return κ, $X^{(\kappa)}$

Table 5.1: Total Least Squares Algorithm

5.2.2 Penalizing Connections using an Information Criterion

As mentioned previously, finding optimal α yields a series of candidate solutions because network structures with more degrees of freedom than the true network have low values for α. In previous work, [1], Akaike's Information Criterion (AIC) was used to penalize the extra connections, where AIC is defined as:

$$AIC = 2k - 2ln(L)$$

where k is the number of parameters in the model and L is the maximized value of the likelihood function for the model.

Akaike's Information Criterion with correction for finite sample sizes is defined as:

$$AICc = AIC + \frac{2k(k+1)}{n-k+1}$$

where n is the sample size.

Applying the AIC to our reconstruction algorithm did not yield good results, since it favored the full Boolean structure too heavily. By observing α values of reconstructed networks, we determined a variation of the AIC that can be used to find the correct Boolean structure. We call this information criterion Vasu's Information Criterion (VIC) and Vasu's

Information Criterion with correction for finite sample sizes (VICc):

$$VIC = 10k + \alpha \tag{5.3}$$

$$VICc = VIC + \frac{10k(k+1)}{n-k-1} \tag{5.4}$$

where k and n are defined the same as in Akaike's Information Criterion.

The coefficients were chosen so as to ensure that structures with large numbers of connections were heavily penalized, while still taking into account the importance of the smallest distance on the discovery of the true structure. Further discussion on how the VIC and VICc was developed is found in Section 7.1

5.3 Robust Reconstruction Examples

We now present several examples for both diagonal and non-diagonal P. Note, in these examples the system is searching for the boolean structure of Q only (we assume the structure of P is known) since it is not unreasonable to assume that you know how you can affect the network.

5.3.1 Example 1: Diagonal P

First, we simulate the linearized single feedback loop from [1] as shown in Figure 5.2, by performing three experiments and perturbing each input.

The linearized state space equations of the single feedback loop are as follows:

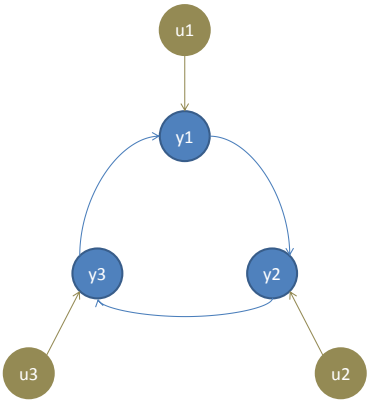

Figure 5.2: Single Feedback Loop with Diagonal P

$$\begin{aligned}
\dot{x_1} &= -x_1 - .2289x_6 + u_1 \\
\dot{x_2} &= -2x_2 + 1.5x_4 + u_2 \\
\dot{x_3} &= -1.5x_3 + 0.5x_5 + u_3 \\
\dot{x_4} &= 0.8x_1 - 0.5x_4 \\
\dot{x_5} &= 1.2x_2 - 0.8x_5 \\
\dot{x_6} &= 1.1x_3 - 1.3x_6
\end{aligned} \tag{5.5}$$

The results of each perturbation experiment are seen in Figure 5.3.

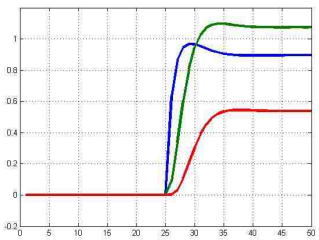

(a) First Perturbation Experiment

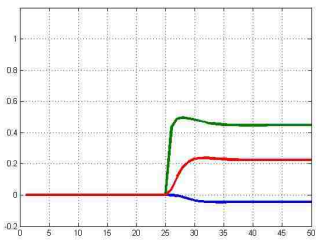

(b) Second Perturbation Experiment

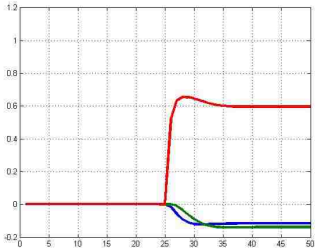

(c) Third Perturbation Experiment

Figure 5.3: Linearized Single Feedback Loop Simulation Results

Running our algorithm, we get the results in Table 5.2, which have been sorted by alpha from largest to smallest. Only a small number of the possible structures are shown in the table since it contains all the relevant data for determining the best structure. The true network is marked in red, while the network chosen using VICc is shown in pink.

Boolean Structure	...	$\begin{bmatrix} 0 & 1 & 0 \\ 1 & 0 & 1 \\ 1 & 1 & 0 \end{bmatrix}$	$\begin{bmatrix} 0 & 0 & 1 \\ 1 & 0 & 0 \\ 0 & 1 & 0 \end{bmatrix}$	$\begin{bmatrix} 0 & 1 & 1 \\ 1 & 0 & 0 \\ 0 & 1 & 0 \end{bmatrix}$	...	$\begin{bmatrix} 0 & 1 & 1 \\ 1 & 0 & 1 \\ 1 & 1 & 0 \end{bmatrix}$
Alpha (α)	...	457.7	0.002166	0.002127	...	2.4×10^{-26}
VICc	...	607.7	54	90	...	270

Table 5.2: Diagonal P without Noise

Note that the $VICc$ is lowest for the correct network. While this is not proof that our algorithm is correct, it is evidence that the robust method works on certain networks when noise is not present in the network. This result is preparatory for a more vigorous analysis, which will be conducted in Chapter 7.

5.3.2 Example 2: Diagonal P with Noise

Using the same linearized single feedback model from Equation 5.5, but with measurement noise added, we get the simulation results seen in Figure 5.4. The noise variance for this test was 1×10^{-3}.

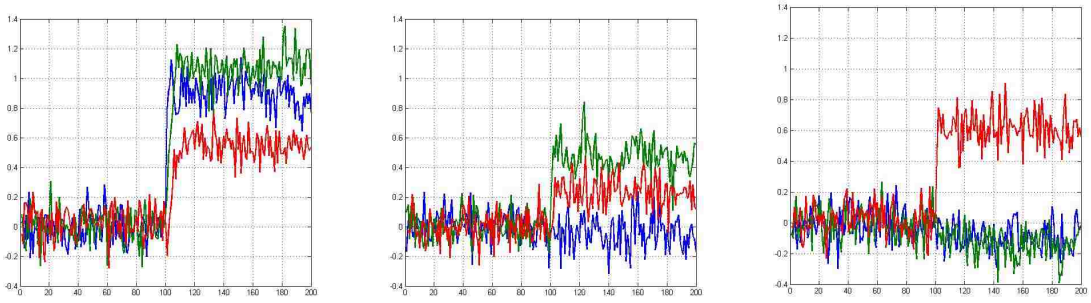

(a) First Perturbation Experiment

(b) Second Perturbation Experiment

(c) Third Perturbation Experiment

Figure 5.4: Linearized Single Feedback Loop with Noise Simulation Results

Running our algorithm, we get the results shown in Table 5.3, which have been sorted by alpha from largest to smallest. Again, only a subset of the candidate structures are shown since it contains all the relevant data needed to determine the best structure. The true network is marked in red and the lowest VICc value is marked in pink.

Boolean Structure	...	$\begin{bmatrix} 0 & 1 & 0 \\ 1 & 0 & 1 \\ 1 & 1 & 0 \end{bmatrix}$	$\begin{bmatrix} 0 & 0 & 1 \\ 1 & 0 & 0 \\ 0 & 1 & 0 \end{bmatrix}$	$\begin{bmatrix} 0 & 1 & 1 \\ 1 & 0 & 0 \\ 0 & 1 & 0 \end{bmatrix}$	...	$\begin{bmatrix} 0 & 1 & 1 \\ 1 & 0 & 1 \\ 1 & 1 & 0 \end{bmatrix}$
Alpha (α)	...	501.5	4.31	4.054	...	5.05×10^{-26}
VICc	...	651.5	58.31	94.05	...	270

Table 5.3: Diagonal P with Noise

The true system still retains the lowest $VICc$ and, as noted previously, while this is not a formal proof or validation that the robust method is correct, it illustrates that the algorithm appears to be working correctly, even when noise is present within the system.

5.3.3 Example 3: Non-Diagonal P

To illustrate that our algorithm works even with non-diagonal P, we begin with something simple, using a slight variation on the simple feedback loop, as can be seen in Figure 5.5.

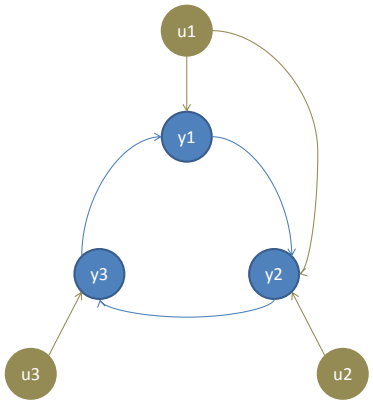

Figure 5.5: Single Feedback Loop with Diagonal P

The state space equations of the non-diagonal P feedback loop are the same as those in Equation (5.5), except for the definition of $\dot{x_2}$ which is defined as:

$$\dot{x_2} = -2x_2 + 1.5x_4 - u_1 + u_2 \tag{5.6}$$

Simulating the system without noise yields the results seen in Figure 5.6.

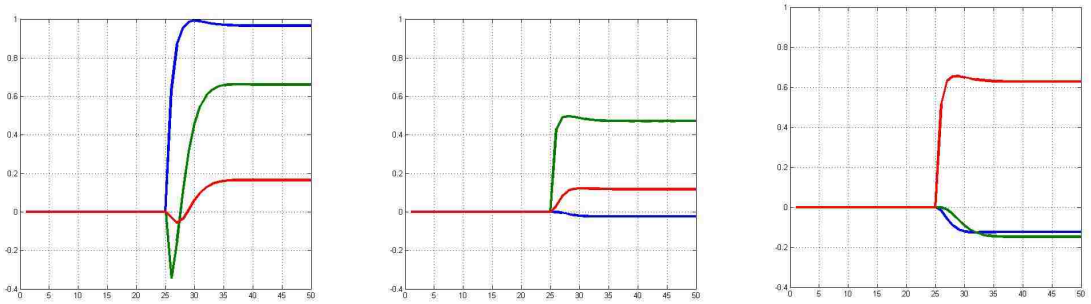

(a) First Perturbation Experiment

(b) Second Perturbation Experiment

(c) Third Perturbation Experiment

Figure 5.6: Linearized Single Feedback Loop with Non-Diagonal P Simulation Results

Running our algorithm, we get the results shown in Table 5.4, which has again been sorted by alpha from largest to smallest. Only relevant data for determining the best structure is shown. The true network is marked in red with the lowest VICc score marked in pink.

Boolean Structure	...	$\begin{bmatrix} 0 & 1 & 0 \\ 1 & 0 & 1 \\ 1 & 1 & 0 \end{bmatrix}$	$\begin{bmatrix} 0 & 0 & 1 \\ 1 & 0 & 0 \\ 0 & 1 & 0 \end{bmatrix}$	$\begin{bmatrix} 0 & 1 & 1 \\ 1 & 0 & 0 \\ 0 & 1 & 0 \end{bmatrix}$	...	$\begin{bmatrix} 0 & 1 & 1 \\ 1 & 0 & 1 \\ 1 & 1 & 0 \end{bmatrix}$
Alpha (α)	...	145.2	0.001528	0.001517	...	8.681×10^{-27}
VICc	...	295.2	54	90	...	270

Table 5.4: Non-Diagonal P without Noise

Note that the $VICc$ is again lowest for the true network, this is promising because we have now shown that our robust results extend beyond the previously reconstructible networks that required P to be diagonal, at least for the example of this network with no noise present.

5.3.4 Non-Diagonal P with Noise

Simulating the system in Equation (5.6) with measurement noise gives us the results seen in Figure 5.7. As in the case with the diagonal P network, the noise variance for this test was 1×10^{-3}.

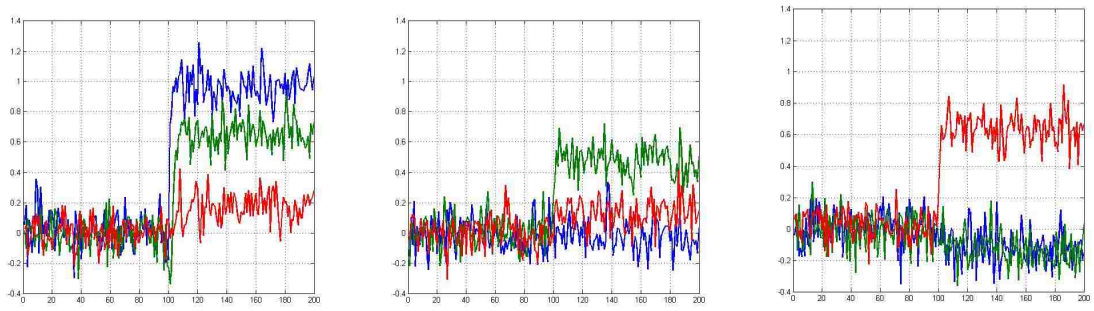

(a) First Perturbation Experiment

(b) Second Perturbation Experiment

(c) Third Perturbation Experiment

Figure 5.7: Linearized Single Feedback Loop with Non-Diagonal P and Noise Simulation Results

Running our algorithm, we get the results shown in Table 5.5, which have again been sorted by alpha from largest to smallest. Only relevant data for determining the best structure is shown. The true network is marked in red and the lowest VICc score is given in pink.

Boolean Structure	...	$\begin{bmatrix} 0 & 1 & 0 \\ 1 & 0 & 1 \\ 1 & 1 & 0 \end{bmatrix}$	$\begin{bmatrix} 0 & 0 & 1 \\ 1 & 0 & 0 \\ 0 & 1 & 0 \end{bmatrix}$	$\begin{bmatrix} 0 & 1 & 1 \\ 1 & 0 & 0 \\ 0 & 1 & 0 \end{bmatrix}$	...	$\begin{bmatrix} 0 & 1 & 1 \\ 1 & 0 & 1 \\ 1 & 1 & 0 \end{bmatrix}$
Alpha (α)	...	168.5	8.301	6.377	...	5.665×10^{-27}
VICc	...	318.5	62.3	96.38	...	270

Table 5.5: Non-Diagonal P with Noise

In this final example, the $AICc$ is again lowest for the true network, so we have shown that for both diagonal and non-diagonal P with and without noise, reconstruction is possible. Before we begin a thorough analysis of the new reconstruction method, we first present the Matlab toolbox that implements the robust network reconstruction algorithm. This Matlab

toolbox was used to generate the examples in this chapter and will be helpful in facilitating an analysis of the reconstruction algorithm.

Chapter 6

Matlab Toolbox

The Matlab toolbox developed for this thesis implements the robust reconstruction algorithm described in Chapter 5. A list of the functions created for this toolbox are outlined in Section 6.1. Then, in Section 6.2 verification of the various functions outlined is conducted. The code fore each of the functions can be found in the Appendix (Chapter 12).

6.1 List of Functions

Table 6.1 contains a list of all the functions that are available in the Matlab toolbox.

Function Name	**Input**	**Output**	**Purpose of Function**
createDiag	Size N	Coefficient cell matrices $Qcoff$ and $Pcoff$, and their corresponding unknowns they multiply, $Qstruct$ and $Pstruct$, along with the total number of unknowns in Q and P, $count1$ and $count2$	This function creates the basic structure constraints for a diagonal P system. Can be edited to create other networks, such as non-diagonal P, easily.

findT	$Qcoff$, $Qstruct$, $Pcoff$, $Pstruct$, $count1$ and $count2$	The a priori information about the network, T	This function takes in a priori information about the network and creates the matrix T
robustRecon	A priori information, T, input-output data, y and u, number of unknowns in Q and P, N and C, flag stating whether or not to display α and $VICc$ values, $displ$	Dynamical Structure Functions Q and P	Given input-output data and a priori information about the network, this function returns the proposed Boolean structure of the network
findAlphas	T, y, u, N	A list of alpha values $aalpha$	Given information about the network, this function returns the alpha values associated with each possible Boolean structure
findCombs	N	List of all possible Boolean structure $allQ$	Creates a list of all possible Boolean structures based on the number of unknowns in Q

getAlpha	T, y, u, $allQ\{i\}$	Alpha α	Given a Boolean structure, this function finds it's α value
zTransform	A vector f and a point on the unit circle z	F, the z-transform of f	Determines the z-transform of a vector f at the point z
findM	Y, U	The matrix M	Given the z-transforms Y and U, we now find M as defined in Equation 5.1 before taking a priori information into account
vectorize	A matrix X	A vector x	Given a matrix, this function turns it into a vector by stacking each row transposed on top of each other
vectorizeCell	A cell matrix X	A vector x	Given a cell matrix, this function turns it into a vector by stacking each row transposed on top of each other
solveAlpha	M and Y	α	Given M and Y, this function returns the value of α

findBest	*aalpha*, N, *displ*, and y	Boolean structure Q	Given all α values, this function returns the proposed Boolean structure for Q
numNonZero	A matrix X	Number of non-zero values in X	Counts the number of non-zero values in a matrix, X, and returns it in the variable N
vicc	$aalpha(i)$, e, the size of Q, and L, the number of non-zero elements of the current structure	VIC and $VICc$	Given L and α for a particular Boolean structure, calculates the VIC and $VICc$ as defined in equations (5.3) and (5.4)
findP	T, C, y, u	Boolean structure P	Given T and the number on unknowns in P, returns the Boolean structure
findQ	T, N, y, u, and $bestX$	Boolean structure Q	Given T and the best Boolean structure as a vector returns the Boolean structure of Q as a matrix

Table 6.1: Functions created for Matlab Toolbox

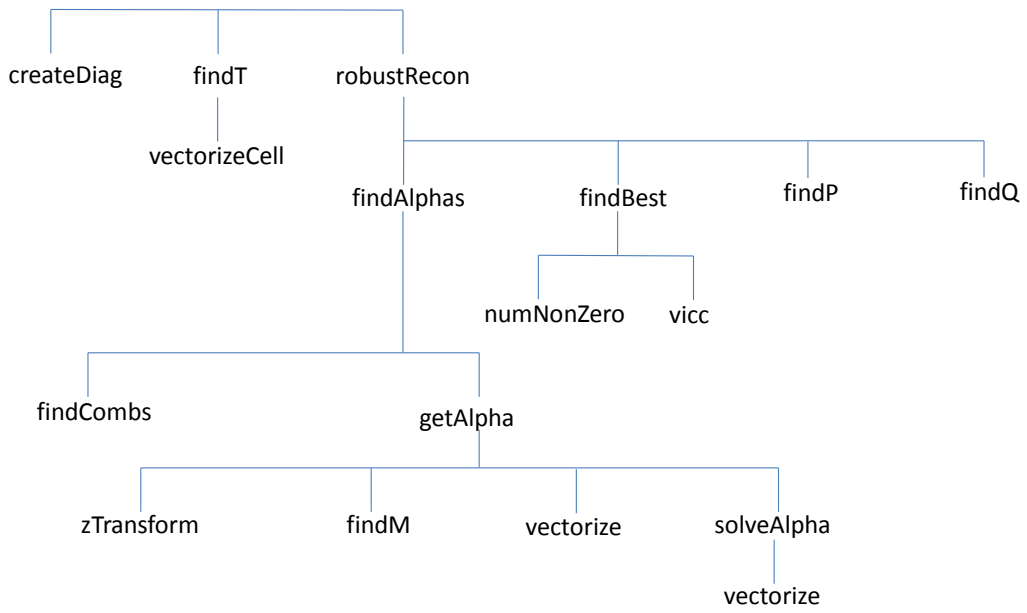

Figure 6.1: Hierarchy of Function Calls in Matlab Toolbox

Figure 6.1 is a decomposition of the Matlab toolbox into all the functions outlined in Table 6.1. The Matlab toolbox implements the robust reconstruction algorithm outlined in Section 5.2.

6.2 Verification of Matlab Toolbox Functions

Function 1: createDiag

Input	Expected Output	Actual Output
-1	Error	Error using createDiag (line 6) You must provide a positive number
0	Error	Error using createDiag (line 6) You must provide a positive number
1	[0], [0], [1], [1], 0, 1	[0], [0], [1], [1], 0, 1
2	$\begin{bmatrix}0 & 1\\1 & 0\end{bmatrix}$, $\begin{bmatrix}0 & 1\\2 & 0\end{bmatrix}$, $\begin{bmatrix}1 & 0\\0 & 1\end{bmatrix}$, $\begin{bmatrix}1 & 0\\0 & 2\end{bmatrix}$, 2, 2	$\begin{bmatrix}0 & 1\\1 & 0\end{bmatrix}$, $\begin{bmatrix}0 & 1\\2 & 0\end{bmatrix}$, $\begin{bmatrix}1 & 0\\0 & 1\end{bmatrix}$, $\begin{bmatrix}1 & 0\\0 & 2\end{bmatrix}$, 2, 2

Table 6.2: Test Cases for function createDiag

Function 2: findT

Input	**Expected Output**	**Actual Output**
$N = 2$, P diagonal, $Qcoff\{1,1\} = [2\ 3]$, $Qstruct\{1,1\} = [1\ 2]$	Error	Error using findT (line 31) Q structure contains non-zero diagonal values.
$Qcoff$ and $Qstruct$ different sizes	Error	Error using findT (line 16) Qcoff and Qstruct must be the same dimensions
$Qcoff$ not square	Error	Error using findT (line 10) Qcoff must be a square matrix
$Qstruct$ not square	Error	Error using findT (line 13) Qstruct must be a square matrix
$Qcoff$ and $Qstruct$ with different number of rows than $Pcoff$ and $Pstruct$	Error	Error using findT (line 25) Pcoff and Pstruct must have the same number of rows as Qcoff and Qstruct
$Pcoff$ and $Pstruct$ different sizes	Error	Error using findT (line 22) Pcoff and Pstruct must be the same dimensions
$N = 1$, P diagonal	[0 1]'	[0 1]'

$N = 2$, P diagonal	$\begin{bmatrix} 0 & 0 & 0 & 0 \\ 1 & 0 & 0 & 0 \\ 0 & 1 & 0 & 0 \\ 0 & 0 & 0 & 0 \\ 0 & 0 & 1 & 0 \\ 0 & 0 & 0 & 0 \\ 0 & 0 & 0 & 0 \\ 0 & 0 & 0 & 1 \end{bmatrix}$	$\begin{bmatrix} 0 & 0 & 0 & 0 \\ 1 & 0 & 0 & 0 \\ 0 & 1 & 0 & 0 \\ 0 & 0 & 0 & 0 \\ 0 & 0 & 1 & 0 \\ 0 & 0 & 0 & 0 \\ 0 & 0 & 0 & 0 \\ 0 & 0 & 0 & 1 \end{bmatrix}$
$N = 2$, P diagonal, $Pcoff\{1,1\} = [1\ 2]$, $Pstruct\{1,1\} = [1\ 2]$	$\begin{bmatrix} 0 & 0 & 0 & 0 \\ 1 & 0 & 0 & 0 \\ 0 & 1 & 0 & 0 \\ 0 & 0 & 0 & 0 \\ 0 & 0 & 1 & 2 \\ 0 & 0 & 0 & 0 \\ 0 & 0 & 0 & 0 \\ 0 & 0 & 0 & 1 \end{bmatrix}$	$\begin{bmatrix} 0 & 0 & 0 & 0 \\ 1 & 0 & 0 & 0 \\ 0 & 1 & 0 & 0 \\ 0 & 0 & 0 & 0 \\ 0 & 0 & 1 & 2 \\ 0 & 0 & 0 & 0 \\ 0 & 0 & 0 & 0 \\ 0 & 0 & 0 & 1 \end{bmatrix}$
$N = 2$, P diagonal, $Pcoff\{1,1\} = [2\ 3]$, $Pstruct\{1,1\} = [1\ 2]$	$\begin{bmatrix} 0 & 0 & 0 & 0 \\ 1 & 0 & 0 & 0 \\ 0 & 1 & 0 & 0 \\ 0 & 0 & 0 & 0 \\ 0 & 0 & 2 & 3 \\ 0 & 0 & 0 & 0 \\ 0 & 0 & 0 & 0 \\ 0 & 0 & 0 & 1 \end{bmatrix}$	$\begin{bmatrix} 0 & 0 & 0 & 0 \\ 1 & 0 & 0 & 0 \\ 0 & 1 & 0 & 0 \\ 0 & 0 & 0 & 0 \\ 0 & 0 & 2 & 3 \\ 0 & 0 & 0 & 0 \\ 0 & 0 & 0 & 0 \\ 0 & 0 & 0 & 1 \end{bmatrix}$

$N = 2$, P diagonal, $Qcoff\{1,2\} = [1\ 2]$, $Qstruct\{1,2\} = [1\ 2]$	$\begin{bmatrix} 0 & 0 & 0 & 0 \\ 1 & 2 & 0 & 0 \\ 0 & 1 & 0 & 0 \\ 0 & 0 & 0 & 0 \\ 0 & 0 & 1 & 0 \\ 0 & 0 & 0 & 0 \\ 0 & 0 & 0 & 0 \\ 0 & 0 & 0 & 1 \end{bmatrix}$	$\begin{bmatrix} 0 & 0 & 0 & 0 \\ 1 & 2 & 0 & 0 \\ 0 & 1 & 0 & 0 \\ 0 & 0 & 0 & 0 \\ 0 & 0 & 1 & 0 \\ 0 & 0 & 0 & 0 \\ 0 & 0 & 0 & 0 \\ 0 & 0 & 0 & 1 \end{bmatrix}$
$N = 2$, P non-diagonal, $Pcoff\{1,2\} = [1\ 2]$, $Pstruct\{1,2\} = [1\ 2]$	$\begin{bmatrix} 0 & 0 & 0 & 0 \\ 1 & 0 & 0 & 0 \\ 0 & 1 & 0 & 0 \\ 0 & 0 & 0 & 0 \\ 0 & 0 & 1 & 0 \\ 0 & 0 & 1 & 2 \\ 0 & 0 & 0 & 0 \\ 0 & 0 & 0 & 1 \end{bmatrix}$	$\begin{bmatrix} 0 & 0 & 0 & 0 \\ 1 & 0 & 0 & 0 \\ 0 & 1 & 0 & 0 \\ 0 & 0 & 0 & 0 \\ 0 & 0 & 1 & 0 \\ 0 & 0 & 1 & 2 \\ 0 & 0 & 0 & 0 \\ 0 & 0 & 0 & 1 \end{bmatrix}$

Table 6.3: Test Cases for function findT

Function 3: robustRecon

Purpose of `robustRecon` is to make function calls to `findAlphas`, `findBest`, `findQ`, and `findP`. No other calculations are performed, so vigorous testing was not required.

Function 4: findAlphas

Purpose of `findAplhas` is to make function calls to `findCombs`, `getAlpha`, `vectorize`, and `sortrows` (a built-in Matlab function). No other calculations are performed, so vigorous testing was not required.

Function 5: findCombs

Input	Expected Output	Actual Output
-1	Error	Error using findCombs (line 4) You must enter a positive number.
0	Error	Error using findCombs (line 4) You must enter a positive number.
1	[0], [1]	[0], [1]
2	[0 0], [0 1], [1 0], [1 1]	[0 0], [0 1], [1 0], [1 1]
3	[0 0 0], [0 1 0], [1 0 0], [1 1 0] [0 0 1], [0 1 1], [1 0 1], [1 1 1]	[0 0 0], [0 1 0], [1 0 0], [1 1 0] [0 0 1], [0 1 1], [1 0 1], [1 1 1]

Table 6.4: Test Cases for function findCombs

Function 6: getAlpha

Purpose of `getAlpha` is to make function calls to `zTransform`, `findM`, `vectorize`, and `solveAplha`. Two calculations are also performed, one chooses points on the unit circle, while the other removes columns of M based on the zero structure of the current Boolean structure being tested. Vigorous testing for each of these calculations are found below:

Find Points on the Unit Circle (input is the number of points, default input is 10)

Input	Expected Output	Actual Output
1	1	1.0000 - 0.0000i
2	1, 1	1, 1.0000 - 0.0000i
3	1,-1,1	1, -1.0000 + 0.0000i, 1.0000 - 0.0000

10	1, .766+0.6428i, .1736+.9848i, -.5+.866i, -.9397+.342i, -.9397 -.342i, -.5-.866i, .1736 - .9848i, .766-.6428i, 1	1, 0.7660+0.6428i, 0.17360+.9848i, -0.5000+0.8660i, -0.9397+0.3420i, -0.9397 -0.3420i, -0.5000-0.8660i, 0.1736 - 0.9848i, 0.7660-0.6428i, 1.0000 - 0.0000i

Table 6.5: Test Cases for function getAlpha: Finding Points on the Unit Circle

Remove Columns of M

Input	**Expected Output**	**Actual Output**
x = zeros(2,1) and M = ones(3,3)	[1 1 1]'	[1 1 1]'
x = ones(2,1) and M = ones(3,3)	$\begin{bmatrix} 1 & 1 & 1 \\ 1 & 1 & 1 \\ 1 & 1 & 1 \end{bmatrix}$	$\begin{bmatrix} 1 & 1 & 1 \\ 1 & 1 & 1 \\ 1 & 1 & 1 \end{bmatrix}$
x = [1 0 1]' and M = [.1*ones(3,1) .2*ones(3,1) .3*ones(3,1)]	$\begin{bmatrix} .1 & .3 \\ .1 & .3 \\ .1 & .3 \end{bmatrix}$	$\begin{bmatrix} .1 & .3 \\ .1 & .3 \\ .1 & .3 \end{bmatrix}$

Table 6.6: Test Cases for function getAlpha: Removing Columns of M

Function 7: zTransform

Input	**Expected Output**	**Actual Output**
X = ones(5,1) and z = 1	5	5
X = ones(5,1) and z = -1	1	1

X = ones(6,1) and z = -1	0	0
X = ones(5,1) and z = .766+.6428i	.4996 - 2.8357i	0.4996 - 2.8357i
X = 2*ones(5,1) and z = .766+.6428i	.9993 - 5.6713i	.9993 - 5.6713i

Table 6.7: Test Cases for function zTransform

Function 8: findM

Input	**Expected Output**	**Actual Output**
Y = ones(2,2) and U 2*ones(2,2)	$\begin{bmatrix} 1 & 1 & 0 & 0 & 2 & 2 & 0 & 0 \\ 1 & 1 & 0 & 0 & 2 & 2 & 0 & 0 \\ 0 & 0 & 1 & 1 & 0 & 0 & 2 & 2 \\ 0 & 0 & 1 & 1 & 0 & 0 & 2 & 2 \end{bmatrix}$	$\begin{bmatrix} 1 & 1 & 0 & 0 & 2 & 2 & 0 & 0 \\ 1 & 1 & 0 & 0 & 2 & 2 & 0 & 0 \\ 0 & 0 & 1 & 1 & 0 & 0 & 2 & 2 \\ 0 & 0 & 1 & 1 & 0 & 0 & 2 & 2 \end{bmatrix}$
Y = ones(2,2) and U 2*ones(3,2)	$\begin{bmatrix} 1 & 1 & 0 & 0 & 2 & 2 & 2 & 0 & 0 & 0 \\ 1 & 1 & 0 & 0 & 2 & 2 & 2 & 0 & 0 & 0 \\ 0 & 0 & 1 & 1 & 0 & 0 & 0 & 2 & 2 & 2 \\ 0 & 0 & 1 & 1 & 0 & 0 & 0 & 2 & 2 & 2 \end{bmatrix}$	$\begin{bmatrix} 1 & 1 & 0 & 0 & 2 & 2 & 2 & 0 & 0 & 0 \\ 1 & 1 & 0 & 0 & 2 & 2 & 2 & 0 & 0 & 0 \\ 0 & 0 & 1 & 1 & 0 & 0 & 0 & 2 & 2 & 2 \\ 0 & 0 & 1 & 1 & 0 & 0 & 0 & 2 & 2 & 2 \end{bmatrix}$
Y = ones(3,2) and U 2*ones(2,2)	$\begin{bmatrix} 1 & 1 & 1 & 0 & 0 & 0 & 2 & 2 & 0 & 0 \\ 1 & 1 & 1 & 0 & 0 & 0 & 2 & 2 & 0 & 0 \\ 0 & 0 & 0 & 1 & 1 & 1 & 0 & 0 & 2 & 2 \\ 0 & 0 & 0 & 1 & 1 & 1 & 0 & 0 & 2 & 2 \end{bmatrix}$	$\begin{bmatrix} 1 & 1 & 1 & 0 & 0 & 0 & 2 & 2 & 0 & 0 \\ 1 & 1 & 1 & 0 & 0 & 0 & 2 & 2 & 0 & 0 \\ 0 & 0 & 0 & 1 & 1 & 1 & 0 & 0 & 2 & 2 \\ 0 & 0 & 0 & 1 & 1 & 1 & 0 & 0 & 2 & 2 \end{bmatrix}$
Y = ones(2,3) and U 2*ones(2,2)	Error	Error using horzcat CAT arguments dimensions are not consistent.

Y = ones(2,2) and U 2*ones(2,3)	Error	Error using horzcat CAT arguments dimensions are not consistent.

Table 6.8: Test Cases for function findM

Function 9: vectorize

Input	Expected Output	Actual Output
ones(2,2)	[1 1 1 1]'	[1 1 1 1]'
ones(2,1)	[1 1]'	[1 1]'
ones(1,2)	[1 1]'	[1 1]'

Table 6.9: Test Cases for function vectorize

Function 10: vectorizeCell

The function `vectorizeCell` is exactly the same as `vectorize` with the constraint that the input must be a cell matrix or vector rather than a normal matrix or vector. Since vigorous testing was conducted on `vectorize`, more testing was not needed here.

Function 11: solveAlpha

Purpose of `solveAplha` is to make function calls to `vectorize`, `pinv` (a built-in Matlab function), and `norm` (another built-in Matlab function). The only other calculation is simple (squaring the norm), so vigorous testing was not required.

Function 12: findBest

Purpose of `findBest` is to find the Boolean structure with the lowest VICc value. This is a trivial operation and does not require vigorous testing.

Function 13: numNonZero

Input	Expected Output	Actual Output
zeros(3,3)	0	0
ones(3,3)	9	9
$\begin{bmatrix} 1 & 2 & 0 \\ -1 & 0 & 4 \\ 0 & 0 & -5 \end{bmatrix}$	5	5
[1 2 0]	2	2
[-1 -2 0]'	2	2

Table 6.10: Test Cases for function numNonZero

Function 14: vicc

Input	Expected Output	Actual Output
$.1, 0, 3$	.1,.1	.1, .1
$1, 6, 4$	61,107.66667	61,107.6667
$10, 20, 25$	210, 216.95364	210, 216.9536

Table 6.11: Test Cases for function vicc

Function 15: findP

Input	Expected Output	Actual Output
T2 = $\begin{bmatrix} 1 & 0 \\ 0 & 0 \\ 0 & 0 \\ 0 & 1 \end{bmatrix}$ size(y) = 2, size(u) = 2, and C = 2	$\begin{bmatrix} 1 & 0 \\ 0 & 1 \end{bmatrix}$	$\begin{bmatrix} 1 & 0 \\ 0 & 1 \end{bmatrix}$

T2 = $\begin{bmatrix} 1 & 0 \\ -1 & 0 \\ 0 & 0 \\ 0 & 1 \end{bmatrix}$ size(y) = 2, size(u) = 2, and C = 2	$\begin{bmatrix} 1 & 1 \\ 0 & 1 \end{bmatrix}$	$\begin{bmatrix} 1 & 1 \\ 0 & 1 \end{bmatrix}$
T2 = $\begin{bmatrix} 1 & 0 \\ 0 & 0 \\ 0 & -1 \\ 0 & 1 \end{bmatrix}$ size(y) = 2, size(u) = 2, and C = 2	$\begin{bmatrix} 1 & 0 \\ 1 & 1 \end{bmatrix}$	$\begin{bmatrix} 1 & 0 \\ 1 & 1 \end{bmatrix}$
T = [T1 0; 0 T2] with T2 = $\begin{bmatrix} 1 & 0 & 0 \\ 0 & 0 & 0 \\ 0 & 0 & 0 \\ 0 & 0 & 0 \\ 0 & 1 & 0 \\ 0 & 0 & 0 \\ 0 & 0 & 0 \\ 0 & 0 & 0 \\ 0 & 0 & 1 \end{bmatrix}$ with size(y) = 3, size(u) = 3, and C = 3	$\begin{bmatrix} 1 & 0 & 0 \\ 0 & 1 & 0 \\ 0 & 0 & 1 \end{bmatrix}$	$\begin{bmatrix} 1 & 0 & 0 \\ 0 & 1 & 0 \\ 0 & 0 & 1 \end{bmatrix}$

Table 6.12: Test Cases for function findP

Function 16: findQ

The function `findQ` is exactly the same as `findP` with the added stipulation that instead of having ones everywhere, the zeros of the proposed Boolean structure is also added. Since vigorous testing was conducted on `findP`, more testing was not needed here.

Chapter 7

Validation and Analysis of Reconstruction Technique

To begin, in Section 7.1 we compare the distance α, characterizing how well a given network structure fits the data, to their corresponding VICc values, penalizing complex network structures, to illustrate why the VICc finds the correct network with low levels of noise on the data. Then, in Section 7.2 we compare the accuracy of the robust reconstruction process as we increase the amount of noise in the network. Finally, in Section 7.3 we introduce the concepts of specificity and sensitivity to determine how close to the actual network we can reconstruct when large amounts of noise are present in the system.

7.1 Comparison of VICc to Distance, α

First, we compare the VICc values to the distance α for each structure in Figure 7.1. These VICc and α values were taken from the linearized single feedback loop with diagonal P with no noise, but non-diagonal P or noise does not change the underlying concepts associated with the comparison.

There are several important things to note, the first being that there are several plateaus and jumps in the figure. Each jump refers to a structure that has included 0's that are not part of the correct network (even if there are 0's in the structure that are part of the correct network). The network with the largest distance is the empty network, while the network with the smallest distance is the full network. This is because the extra degrees of freedom ensure that the value for α is low. The correct network structure is the value at the

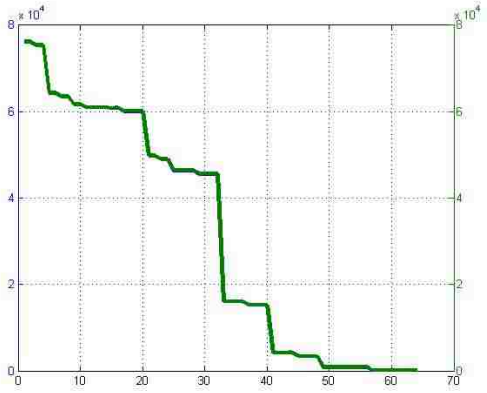

Figure 7.1: Comparing VICc to α Values

left end of the first plateau, since that plateau contains all the correct zeros of the network and anything on that plateau has zeros in the correct spot, with extra degrees of freedom somewhere.

Now it is difficult to see the difference between the α values and the VICc values from Figure 7.1, so in Figure 7.2 we focus on the first plateau. The α values are in blue, with the VICc values in green. As the figure shows, the first plateau in blue increases as alpha increases as the structure loses degrees of freedom, until it reaches the correct network and then jumps up to a much higher value. The purpose of the VICc is to penalize these extra defrees of freedom, so instead of an increasing line, the compensation for extra connections causes the green line to decrease until it reaches the correct network, before jumping up to a higher value.

So, while the VICc values don't guarantee reconstruction, we can see how with small amounts of noise, they make reconstruction possible.

7.2 Accuracy of Robust Reconstruction

To test exactly how much noise the system can handle, we turn to Figure 7.3, which shows the accuracy of the reconstruction, which refers to what percentage of 100 attempts to reconstruct yielded the correct Boolean structure, as we increase noise variance. The experiments were

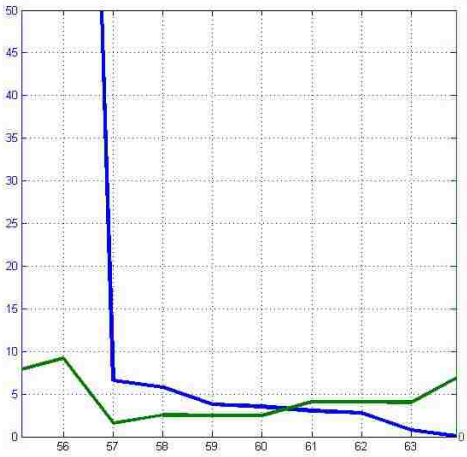

Figure 7.2: Closer Inspection of VICc and α Comparison

conducted on the single feedback loop with non-diagonal P, although the analysis is general enough that it should apply to all reconstructed networks.

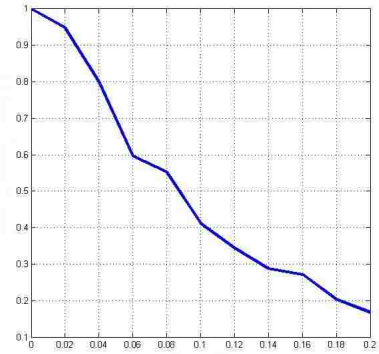

Figure 7.3: Accuracy of Reconstruction with increasing Noise Variance

As the figure shows, the accuracy steadily decreases as the noise variance increases, which is as expected. As the noise variance gets too large, the α value for the correct network gets larger, while the α values for the networks with more degrees of freedom grow slower.

One way to counteract the decreasing accuracy is to include noise averaging, which relies on running the experiments multiple times to reduce the effects of noise on the network. Doing this, we get the results shown in Figure 7.4. As the figure shows, with 2×10^{-3} noise variance, the accuracy has increased from below 20% to around 75%. Therefore, although

the accuracy is still decreasing over time, the rate of decay is drastically reduced by using noise averaging.

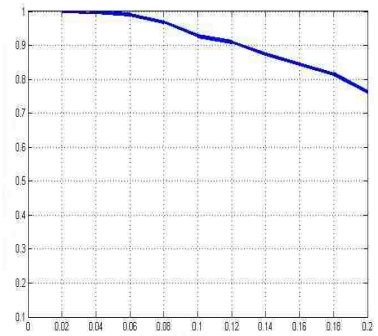

Figure 7.4: Accuracy of Reconstruction using Noise Averaging

As noise variance increases and the accuracy of perfect reconstruction of the Boolean structure becomes poorer, we may want to ask, how close to the actual network are we reconstructing?

7.3 Specificity and Sensitivity of Robust Reconstruction Technique

Thus, we can introduce the notions of specificity, the ability to accurately discern where the absence of a reaction is, and sensitivity, the ability to detect the incidence of a reaction between two species. To test this, we chose a noise variance of 2×10^{-3} without noise averaging, which in our examples means the network reconstructs correctly *most* of the time (around $70 - 80\%$ accuracy). We want to evaluate how close to the correct network we get when we don't correctly reconstruct. To do this we created random networks with three nodes, to ensure that we captured the entire scope of possible networks, we generated every possible network of three nodes, starting with an empty network all the way to a full network. To improve the accuracy of our results, we also ran each type of network 100 times.

The results we obtained were as follows: the accuracy was 69.39%, the specificity was 82.16%, and the sensitivity was 99.09%. Firstly, we note that we were only able to reconstruct the Boolean structure perfectly about 70% of the time, due to the amount of noise in the

system. Comparing the sensitivity to the specificity, we see that when we didn't reconstruct correctly, it was more likely because we couldn't detect the absence of a reaction more often than the fact that we couldn't correctly identify a reaction. This was expected since our α values tend to favor networks with higher degrees of freedom. So, when the noise variance increases, the correct network's VICc value starts to lose more often to networks with higher degrees of freedom.

Chapter 8

Applications to Biological Networks

The motivation for extending the reconstruction method to include networks with non-diagonal P was the network known as the Per-Arnt-Sim (PAS) Kinase pathway, which is being studied by Julianne Grose and John Prince in the Biology and Biochemistry departments at Brigham Young University. The PAS Kinase pathway is an important and interesting application for network reconstruction because human mutations in the PAS Kinase pathway have recently been linked to the early development of type 2 diabetes [71].

In Section 8.1 we describe in detail the machanics of the PAS Kinase network. A theoretical reconstruction of the PAS Kinase network is then performed in Section 8.2. Finally, simulations of the PAS Kinase network were conducted and Section 8.3 provides results and analysis.

8.1 PAS Kinase Pathway

The PAS Kinase pathway is composed of proteins that interact in specific ways to direct the metabolism of sugars in eukaryotic cells. Each of these proteins have both an activated and a deactivated form that serves a distinct function within the network. The identification of network structure in this system is an ideal application of signal structure theory. Several PAS Kinase networks have been proposed such as in [72], so analysis of such a pathway with the dynamical structure function method would help to indicate flaws or validate proposed biological pathways. Yeast serves as a model biological organism for understanding the basic

processes of life due to the ease of study and the conservation of many pathways. In fact, the best characterized PAS Kinase pathway, the Ugp1 pathway, was first identified in yeast [73].

One of the proposed networks for the PAS Kinase Ugp1 pathway is indicated in Fig. 1. In this pathway there are three proteins that are directly formed from a gene: PSK, Ugp1, and Glc7; the others are activated forms or complexes involving these three proteins. The species of interest in the pathway are Ugp1, Ugp1* and the Ugp1*Glc7. The asterisk (Upg1*) implies an activated form of Ugp1 that is produced when PAS Kinase modifies the Ugp1 protein [73]. Once Ugp1 is activated, it partitions the use of cellular glucose towards structural components at the expense of storage carbohydrates [74].

The last species, Ugp1*Glc7, is theoretical and may be formed by a direct interaction between Ugp1* and Glc7 [73]. It is hypothesized that Ugp1* is deactivated by this process, however this needs to be verified. Other key network players include the Snf1 protein, which is required for the activation of PAS Kinase in response to available nutrients [75].

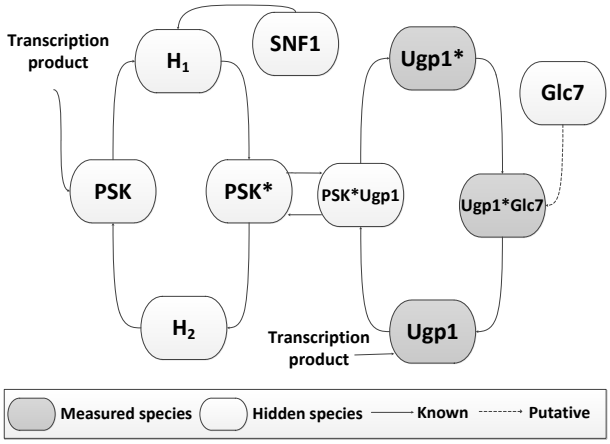

Figure 8.1: PAS Kinase Pathway with H_1 and H_2 representing networks of unobserved nodes

As shown, the current theoretical network involves ten species, with the majority of the pathway verified. It is not easy to directly perturb each of the three nodes of interest since PSK affects two of the observed nodes however, it is possible to create experiments that directly affect two of the species, meaning P is not diagonal. These experiments consist of turning on or off a specified gene by modifying the yeast cell or its environment. This is

commonly done through the use of a plasmid, a small circular piece of DNA inserted into the yeast cell that expresses the protein in response to external stimulus (such as the addition of a particular chemical to the growth media).

The experiments for the PAS kinase network include manipulation of the genes Glc7, Ugp1, and PSK. The plasmids with Glc7 and PSK will directly affect two observed nodes: Ugp1* and Ugp1. However, this will be done in an equal amount; it will increase the activated form of Ugp1* while decreasing the inactive form, Ugp1 . The experimental setup is shown below in Fig. 8.2.

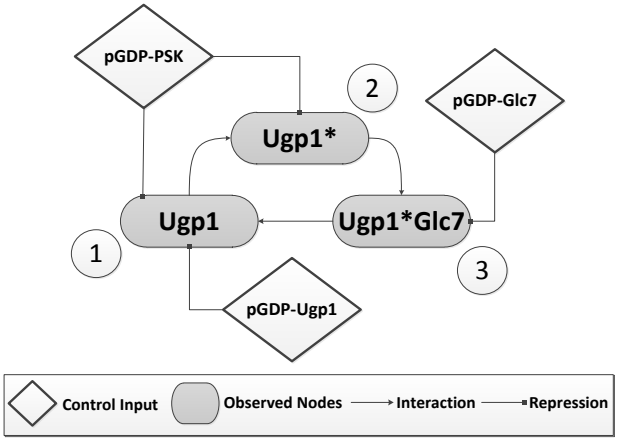

Figure 8.2: Experimental setup for PAS Kinase Pathway

As expected, the exact mechanisms by which phosphorylation and dephosphorylation occur are hidden in this formulation. As indicated earlier, previous formulation required a direct perturbation for each observed node in any given network. However, methods or experimental conditions that independently perturb observed nodes in biological networks are usually not feasible. This becomes even more difficult to do when biological networks have several observed nodes; in many cases it is even impossible to independently perturb all the observed nodes.

However, as the new necessary and sufficient conditions shown in this thesis have indicated, reconstruction is still possible despite multiple perturbations of observed nodes in

a given experiment. This is demonstrated for the PAS Kinase pathway as indicated in Fig. 8.2.

8.2 Reconstruction for PAS Kinase Pathway

From Fig. 8.2, we can define Q, P, and G for the pathway as follows:

$$G_{PAS} = \begin{bmatrix} G_1 & G_2 & G_3 \\ G_4 & G_5 & G_6 \\ G_7 & G_8 & G_9 \end{bmatrix} \tag{8.1}$$

$$Q_{PAS} = \begin{bmatrix} 0 & Q_1 & Q_2 \\ Q_3 & 0 & Q_4 \\ Q_5 & Q_6 & 0 \end{bmatrix} \tag{8.2}$$

$$P_{PAS} = \begin{bmatrix} P_1 & P_2 & P_3 \\ P_4 & P_5 & P_6 \\ P_7 & P_8 & P_9 \end{bmatrix} \tag{8.3}$$

However, from the experimental design indicated in Fig. 8.2, we know the true representation of the control matrix P is as follows:

$$P_{PAS} = \begin{bmatrix} -P_{PSK} & P_{Ugp1} & 0 \\ P_{PSK} & 0 & 0 \\ 0 & 0 & P_{Glc7} \end{bmatrix}$$

Where $P_{PSK} = P_1, P_{Ugp1} = P_2$, and$P_{Glc7} = P_9$.This true representation of P serves as the prior knowledge for this system. Given $L\vec{x} = \vec{b}$ such that:

$$\left[\begin{array}{c|cccccc} & G_4 & G_7 & 0 & 0 & 0 & 0 \\ & G_5 & G_8 & 0 & 0 & 0 & 0 \\ & G_6 & G_9 & 0 & 0 & 0 & 0 \\ & 0 & 0 & G_1 & G_7 & 0 & 0 \\ \mathrm{I} & 0 & 0 & G_2 & G_8 & 0 & 0 \\ & 0 & 0 & G_3 & G_9 & 0 & 0 \\ & 0 & 0 & 0 & 0 & G_1 & G_4 \\ & 0 & 0 & 0 & 0 & G_2 & G_5 \\ & 0 & 0 & 0 & 0 & G_3 & G_6 \end{array}\right] \times \begin{bmatrix} P_1 \\ P_2 \\ \vdots \\ P_9 \\ Q_1 \\ \vdots \\ Q_6 \end{bmatrix} = \begin{bmatrix} G_1 \\ G_2 \\ \vdots \\ G_9 \end{bmatrix}$$

This system has 15 unknowns and 9 equations, so it is easy to see that no unique solution exists as is. However, taking into account a priori information given the true structure of P, we can decompose $\vec{x}$ into $T\vec{z}$ as follows:

$$T = \begin{bmatrix} 1 & 0 & 0 & 0 & 0 & 0 & 0 & 0 & 0 \\ 0 & 1 & 0 & 0 & 0 & 0 & 0 & 0 & 0 \\ 0 & 0 & 0 & 0 & 0 & 0 & 0 & 0 & 0 \\ -1 & 0 & 0 & 0 & 0 & 0 & 0 & 0 & 0 \\ 0 & 0 & 0 & 0 & 0 & 0 & 0 & 0 & 0 \\ 0 & 0 & 0 & 0 & 0 & 0 & 0 & 0 & 0 \\ 0 & 0 & 0 & 0 & 0 & 0 & 0 & 0 & 0 \\ 0 & 0 & 0 & 0 & 0 & 0 & 0 & 0 & 0 \\ 0 & 0 & 1 & 0 & 0 & 0 & 0 & 0 & 0 \\ 0 & 0 & 0 & 1 & 0 & 0 & 0 & 0 & 0 \\ 0 & 0 & 0 & 0 & 1 & 0 & 0 & 0 & 0 \\ 0 & 0 & 0 & 0 & 0 & 1 & 0 & 0 & 0 \\ 0 & 0 & 0 & 0 & 0 & 0 & 1 & 0 & 0 \\ 0 & 0 & 0 & 0 & 0 & 0 & 0 & 1 & 0 \\ 0 & 0 & 0 & 0 & 0 & 0 & 0 & 0 & 1 \end{bmatrix} \quad \text{and } \vec{z} = \begin{bmatrix} P_1 \\ P_2 \\ P_9 \\ Q_1 \\ \vdots \\ Q_6 \end{bmatrix}$$

The total number of variables in $\vec{z}$ is 9, and T is full column rank. In this case, $k = pm$, given $M\vec{z} = \vec{b}$ ($M = LT$), and since M is square and full rank, $(M)^{-1}$ exists. Therefore, $\vec{z} = (M)^{-1}\vec{b}$, hence reconstrcution is possible, and the signal structure of the system can be uniquely identified from the overall structure of Q

8.3 Simulation of the PAS Kinase Pathway

Since we don't have chemical kinetic equations that describe the PAS Kinase Pathway, in order to simulate the system, we generated 10,000 random networks that had similar features to the PAS Kinase Pathway and simulated those with a noise variance of 2×10^{-3} without noise averaging.

The accuracy of this process was 77.58%, the specificity was 93.97% and the sensitivity was 97.34%. These results show that even when we can't reconstruct correctly, there is a high chance that we can reconstruct close to the correct network. Furthermore, utilizing noise averaging would greatly increase the accuracy of our results.

Discussions with biologists have shown that the amount of noise used in our simulations is likely much more than the noise we are likely to see in data from real experiments. This means that there is a high chance that we will be able to reconstruct correctly given data from perturbation experiments.

Chapter 9

Applications to Wireless Networks

We now use the differential model of the MAC presented in Section 1.1 to show that the DSF of the system changes when interfering devices are physically present in a wireless network. Whenever new wireless devices intrude on an existing network, the map changes because of the coupling it creates. Since the map is easy to create, whenever the performance of the links changes, we can recalculate the map in order to examine the network for possible interference from transitory devices. These devices could be other computers with WiFi interfaces or any device that emits an RF signal on the same frequency as the managed WiFi network. Section 9.1 discusses the procedure for determining an initial dynamic interference map of the network. Using the map, we note in Section 9.2 how external intruders or interferers can cause the map to change and thereby be detected.

9.1 Reconstruction Without Transitory Interference

Consider the wireless network as shown in Figure 9.1a, but without link 4 present. The contention graph for this network is given in Figure 9.1b, but without the node 4 and without any of the edges connected to node 4. We show how to derive the exact DSF for this network, assuming we know the differential equation model for the MAC. This will provide a "ground truth" for the network, which the reconstruction algorithm should match.

For this network, the equations describing the rates obtained by these links are given by:

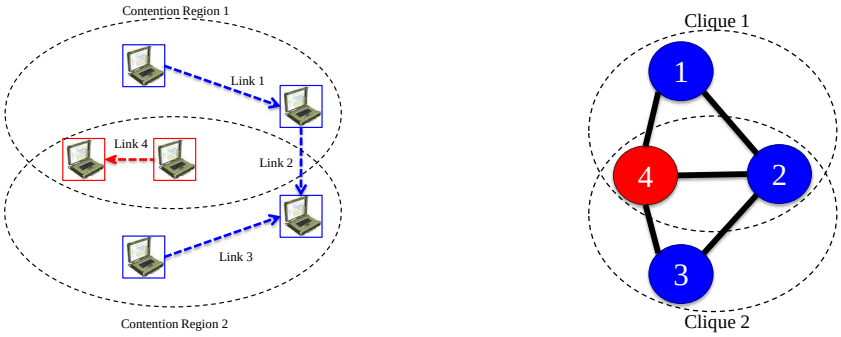

(a) Topology (b) Contention graph

Figure 9.1: Example wireless network, with transitory devices shown in red, along with corresponding contention graph.

$$\begin{bmatrix} \dot{b_1} \\ \dot{b_2} \\ \dot{b_3} \end{bmatrix} = \begin{bmatrix} u_1 - x_1 \\ u_2 - x_2 \\ u_3 - x_3 \end{bmatrix} \tag{9.1}$$

$$\begin{bmatrix} \dot{x_1} \\ \dot{x_2} \\ \dot{x_3} \end{bmatrix} = \begin{bmatrix} -x_1 + \beta_1 \sigma(b_1) \left(x_1 + (1-x_1) \left(1 - \frac{x_2}{1-x_1} \right) \right) \\ -x_2 + \beta_2 \sigma(b_2) \left(x_2 + (1-x_2) \left(1 - \frac{x_1}{1-x_2} \right) \left(1 - \frac{x_3}{1-x_2} \right) \right) \\ -x_3 + \beta_3 \sigma(b_3) \left(x_3 + (1-x_3) \left(1 - \frac{x_2}{1-x_3} \right) \right) \end{bmatrix}$$

Assume that a rate controller is being used on all the links to give fair network performance. The equilibrium rates for this network are $u_1 = 0.4$, $u_2 = 0.4$, and $u_3 = 0.4$. We linearize the system of equations in (9.1) around this equilibrium to get:

$$\begin{bmatrix} \dot{x_1} \\ \dot{x_2} \\ \dot{x_3} \\ \dot{b_1} \\ \dot{b_2} \\ \dot{b_3} \end{bmatrix} = \begin{bmatrix} -1 & -0.66 & 0 & 0.11 & 0 & 0 \\ -0.29 & -0.62 & -0.29 & 0 & 0.02 & 0 \\ 0 & -0.66 & -1 & 0 & 0 & 0.11 \\ -1 & 0 & 0 & 0 & 0 & 0 \\ 0 & -1 & 0 & 0 & 0 & 0 \\ 0 & 0 & -1 & 0 & 0 & 0 \end{bmatrix} \begin{bmatrix} x_1 \\ x_2 \\ x_3 \\ b_1 \\ b_2 \\ b_3 \end{bmatrix} + \begin{bmatrix} 0 & 0 & 0 \\ 0 & 0 & 0 \\ 0 & 0 & 0 \\ 1 & 0 & 0 \\ 0 & 1 & 0 \\ 0 & 0 & 1 \end{bmatrix} \begin{bmatrix} u_1 \\ u_2 \\ u_3 \end{bmatrix}$$

$$\begin{bmatrix} y_1 \\ y_2 \\ y_3 \end{bmatrix} = \begin{bmatrix} 1 & 0 & 0 & 0 & 0 & 0 \\ 0 & 1 & 0 & 0 & 0 & 0 \\ 0 & 0 & 1 & 0 & 0 & 0 \end{bmatrix} \begin{bmatrix} x_1 \\ x_2 \\ x_3 \\ b_1 \\ b_2 \\ b_3 \end{bmatrix}$$

The exact (Q, P) for this system is:

$$Q = \begin{bmatrix} 0 & -\frac{66\,s}{100\,s^2+100\,s+11} & 0 \\ -\frac{29\,s}{2\left(50\,s^2+31\,s+1\right)} & 0 & -\frac{29\,s}{2\left(50\,s^2+31\,s+1\right)} \\ 0 & -\frac{66\,s}{100\,s^2+100\,s+11} & 0 \end{bmatrix}, \text{ and}$$

$$P = \begin{bmatrix} \frac{11}{100\,s^2+100\,s+11} & 0 & 0 \\ 0 & \frac{1}{50\,s^2+31\,s+1} & 0 \\ 0 & 0 & \frac{11}{100\,s^2+100\,s+11} \end{bmatrix}.$$

A graphical representation of this DSF is shown in Figure 9.2a.

(a) Before intrusion (b) After intrusion

Figure 9.2: Structure of the DSF before and after intrusion.

In practical situations, it is not possible to know the system of differential equations that describe the wireless network. In this case, we must use the robust reconstruction method described in Chapter 5 to determine the Boolean structure of the DSF.

For our example, we simulated the nonlinear system with noise in order to get a response similar to that of a real wireless network. First, we perturb each link and record the measurements of each perturbation experiment. The results of these experiments are shown in Figure 9.3. Then, using the noisy data that is collected, find the total least squares solution, α_k, for all possible boolean structures. Note that since we know the structure is symmetric (because if link i interferes with link j, it is obvious that link j interferes with link i), we only need to search over eight possible structures. The results are in Table 9.1, along with their associated $VICc$ values.

In Table 9.1, we see that although the correct structure, marked in red, does not have the lowest α score, by using $VICc$ we can discriminate against structures with more non-zero elements to determine the correct structure. The lowest VICc score is marked in pink.

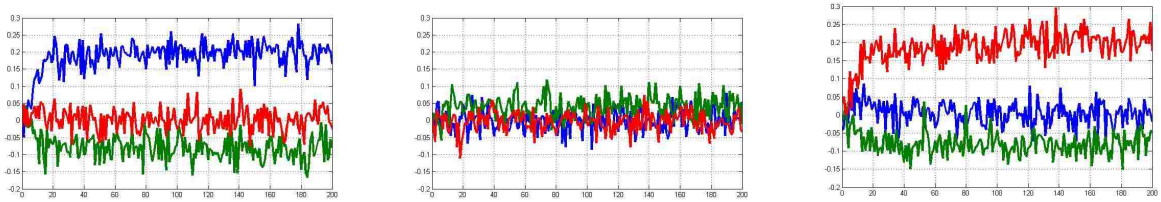

(a) Perturbation on Link 1 (b) Perturbation on Link 2 (c) Perturbation on Link 3

Figure 9.3: Perturbation Experiments for Wireless Network without Transitory Interference

Results of Reconstruction Process		
Boolean Structure	**alpha**	**VICc**
$\begin{bmatrix} 0 & 0 & 0 \\ 0 & 0 & 0 \\ 0 & 0 & 0 \end{bmatrix}$	489.1	489.1
$\begin{bmatrix} 0 & 0 & 1 \\ 0 & 0 & 0 \\ 1 & 0 & 0 \end{bmatrix}$	488.7	518.7
$\begin{bmatrix} 0 & 0 & 0 \\ 0 & 0 & 1 \\ 0 & 1 & 0 \end{bmatrix}$	241.6	271.6
$\begin{bmatrix} 0 & 0 & 1 \\ 0 & 0 & 1 \\ 1 & 1 & 0 \end{bmatrix}$	241.2	331.2
$\begin{bmatrix} 0 & 1 & 0 \\ 1 & 0 & 0 \\ 0 & 0 & 0 \end{bmatrix}$	237.4	267.4
$\begin{bmatrix} 0 & 1 & 1 \\ 1 & 0 & 0 \\ 1 & 0 & 0 \end{bmatrix}$	237.3	327.3
$\begin{bmatrix} 0 & 1 & 0 \\ 1 & 0 & 1 \\ 0 & 1 & 0 \end{bmatrix}$	1.304	91.3
$\begin{bmatrix} 0 & 1 & 1 \\ 1 & 0 & 1 \\ 1 & 1 & 0 \end{bmatrix}$	0.06828	270.1

Table 9.1: Reconstruction Without Transient Interference

9.2 Reconstruction With Transitory Interference

Now let us assume that new network devices begin operating within the contention region of our original network, creating link 4 as shown in Figure 9.1a. The nonlinear model of this network is given by:

$$\begin{bmatrix} \dot{b_1} \\ b_2 \\ b_3 \\ b_4 \end{bmatrix} = \begin{bmatrix} u_1 - x_1 \\ u_2 - x_2 \\ u_3 - x_3 \\ u_4 - x_4 \end{bmatrix} \tag{9.2}$$

$$\dot{x}_1 = -x_1 + \beta_1 \sigma(b_1)\left(x_1 + (1-x_1)\left(1 - \frac{x_2+x_4}{1-x_1}\right)\right)$$

$$\dot{x}_2 = -x_2 + \beta_2 \sigma(b_2)\left(x_2 + (1-x_2)(1-x_4)\left(1 - \frac{x_1}{1-x_2-x_4}\right)\left(1 - \frac{x_3}{1-x_2-x_4}\right)\right)$$

$$\dot{x}_3 = -x_3 + \beta_3 \sigma(b_3)\left(x_3 + (1-x_3)\left(1 - \frac{x_2+x_4}{1-x_3}\right)\right)$$

$$\dot{x}_4 = -x_4 + \beta_4 \sigma(b_4)\left(x_4 + (1-x_2)(1-x_4)\left(1 - \frac{x_1}{1-x_2-x_4}\right)\left(1 - \frac{x_3}{1-x_2-x_4}\right)\right)$$

The new devices decide to set their load to $u_4 = 0.2$. This gives them the equilibrium sending rates of $x_4 = 0.2$. To keep the buffer from growing too large, link 2 has to recalibrate its sending rate to $u_2 = 0.2$ decreasing its rate to 0.2. Linearizing around the new equilibrium,

$$\begin{bmatrix} b_1 & b_2 & b_3 & b_4 & x_1 & x_2 & x_3 & x_4 \end{bmatrix} = \begin{bmatrix} 1 & 1.5 & 1 & 1.5 & 0.4 & 0.2 & 0.4 & 0.2 \end{bmatrix}$$

yields:

$$\begin{bmatrix} \dot{x_1} \\ x_2 \\ x_3 \\ x_4 \\ b_1 \\ b_2 \\ b_3 \\ b_4 \end{bmatrix} = \begin{bmatrix} -1 & -0.66 & 0 & -0.66 & 0.11 & 0 & 0 & 0 \\ -0.26 & -0.68 & -0.26 & -0.41 & 0 & 0.04 & 0 & 0 \\ 0 & -0.66 & -1 & -0.66 & 0 & 0 & 0.11 & 0 \\ -0.26 & -0.41 & -0.26 & -0.68 & 0 & 0 & 0 & 0.04 \\ -1 & 0 & 0 & 0 & 0 & 0 & 0 & 0 \\ 0 & -1 & 0 & 0 & 0 & 0 & 0 & 0 \\ 0 & 0 & -1 & 0 & 0 & 0 & 0 & 0 \\ 0 & 0 & 0 & -1 & 0 & 0 & 0 & 0 \end{bmatrix} \begin{bmatrix} x_1 \\ x_2 \\ x_3 \\ x_4 \\ b_1 \\ b_2 \\ b_3 \\ b_4 \end{bmatrix} + \begin{bmatrix} 0 & 0 & 0 & 0 \\ 0 & 0 & 0 & 0 \\ 0 & 0 & 0 & 0 \\ 0 & 0 & 0 & 0 \\ 1 & 0 & 0 & 0 \\ 0 & 1 & 0 & 0 \\ 0 & 0 & 1 & 0 \\ 0 & 0 & 0 & 1 \end{bmatrix} \begin{bmatrix} u_1 \\ u_2 \\ u_3 \\ u_4 \end{bmatrix}$$

$$\begin{bmatrix} y_1 \\ y_2 \\ y_3 \end{bmatrix} = \begin{bmatrix} 1 & 0 & 0 & 0 & 0 & 0 & 0 & 0 \\ 0 & 1 & 0 & 0 & 0 & 0 & 0 & 0 \\ 0 & 0 & 1 & 0 & 0 & 0 & 0 & 0 \end{bmatrix} \begin{bmatrix} x_1 \\ x_2 \\ x_3 \\ x_4 \\ b_1 \\ b_2 \\ b_3 \\ b_4 \end{bmatrix}$$

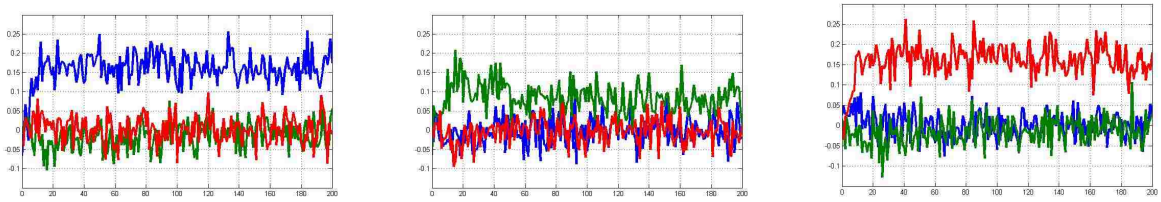

(a) Perturbation on Link 1 (b) Perturbation on Link 2 (c) Perturbation on Link 3

Figure 9.4: Perturbation Experiments for Wireless Network with Transitory Interference

The new DSF, using the inputs on nodes 1, 2, and 3, is given by:

$$Q_2 = \begin{bmatrix} 0 & -\frac{33s\left(100s^2+27s+4\right)}{2(d(s))} & \frac{429s^2}{d(s)} \\ -\frac{26s}{100s^2+109s+4} & 0 & -\frac{26s}{100s^2+109s+4} \\ \frac{429s^2}{d(s)} & -\frac{33s\left(100s^2+27s+4\right)}{2(d(s))} & 0 \end{bmatrix},$$

and

$$P_2 = \begin{bmatrix} \frac{275s^2+187s+11}{d(s)} & 0 & 0 \\ 0 & \frac{2}{100s^2+27s+4}+\frac{2}{100s^2+109s+4} & 0 \\ 0 & 0 & \frac{275s^2+187s+11}{d(s)} \end{bmatrix}$$

where $d(s) = 2500s^4 + 4200s^3 + 1646s^2 + 287s + 11$.

Again, these dynamical structure functions (Q, P) have been determined directly from the differential equations. We will now assume that the differential equations that describe the wireless network are unknown, and we will use the robust reconstruction process from Chapter 5 to determine the boolean structure of the network while the interference is occurring.

As before, we first perturb each link and record the measurements of each perturbation experiment. The results of these experiments are shown in Figure 9.4. Then, using the noisy data that is collected, find the total least squares solution, α_k, for all possible Boolean structures. The results are in Table 9.2, along with their associated $VICc$ values.

As we can now see, the correct structure, marked in red in Table 9.2, is now the fully connected network, with the lowest VICc value marked in pink. A graphical representation

Results of Reconstruction Process		
Boolean Structure	**alpha**	**AIC**
$\begin{bmatrix} 0 & 0 & 0 \\ 0 & 0 & 0 \\ 0 & 0 & 0 \end{bmatrix}$	6844	6844
$\begin{bmatrix} 0 & 0 & 1 \\ 0 & 0 & 0 \\ 1 & 0 & 0 \end{bmatrix}$	5039	5069
$\begin{bmatrix} 0 & 1 & 0 \\ 1 & 0 & 0 \\ 0 & 0 & 0 \end{bmatrix}$	4727	4757
$\begin{bmatrix} 0 & 0 & 0 \\ 0 & 0 & 1 \\ 0 & 1 & 0 \end{bmatrix}$	4705	4735
$\begin{bmatrix} 0 & 1 & 0 \\ 1 & 0 & 1 \\ 0 & 1 & 0 \end{bmatrix}$	2608	2698
$\begin{bmatrix} 0 & 1 & 1 \\ 1 & 0 & 0 \\ 1 & 0 & 0 \end{bmatrix}$	2511	2601
$\begin{bmatrix} 0 & 0 & 1 \\ 0 & 0 & 1 \\ 0 & 1 & 1 \end{bmatrix}$	2506	2596
$\begin{bmatrix} 0 & 1 & 1 \\ 1 & 0 & 1 \\ 1 & 1 & 0 \end{bmatrix}$	0.00003131	270

Table 9.2: Reconstruction With Transient Interference

of this DSF is shown in Figure 9.2b. We can see that the links 1 and 3 were not coupled in Figure 9.2a, but now they appear coupled. This signals the presence of interfering wireless devices.

If the new devices do not create new links in the DSF, but do change the transfer functions contained in Q and P, then the presence of such an intruder is harder to detect.

Chapter 10

Overview of Contributions and Future Work with Dynamical Structure Functions

To conclude this thesis we now present an overview of the major contributions of this thesis as well as discussing ideas for future work based upon the progress of this thesis.

10.1 Major Contribution 1: Necessary and Sufficient Identifiability Conditions

The first contribution of this thesis was to develop necessary and sufficient informativity condtions for the reconstruction of a network. This allows for reconstruction even when each measured state cannot be independently controlled by an input. This was an important contribution because it increased the applicability of network reconstruction with dynamical structure functions to networks that were not previously known to be reconstructible.

The necessary and sufficient informativity conditions are detailed in Chapter 4, the specific theorem stating the necessary and sufficient conditions for perfect reconstruction was Theorem 3, which stated that given a system characterized by the transfer function G, its dynamical structure function (Q, P) can be identified if and only if

1. M, defined as in Equation (4.6), is injective, and
2. $\overleftarrow{g} \in \mathcal{R}(M)$.

where $\overleftarrow{g}$ is the vector stack of the columns of G', the conjugate transpose of the transfer function matrix.

10.2 Major Contribution 2: Robust Reconstruction Algorithm for Networks with Non-Diagonal P

The second major contribution of this thesis spawned from the creation of the new necessary and sufficient informativity conditions for network reconstruction using dynamical structure functions. Previous robust reconstruction methods were based upon the assumption that P was diagonal. The new conditions showed that this was not always the case, so a new robust reconstruction method was required.

The method seeks to minimize Δ, which represents the additive noise and nonlinearities on P. We showed that this was equivalent to minimizing the norm $||Y - \begin{bmatrix} Q & P \end{bmatrix} \begin{bmatrix} Y \\ U \end{bmatrix} ||$, which could be rearranged into a total least squares problem. The algorithm for solving the robust reconstruction problem is to solve this total least squares problem for every possible Boolean structure of Q and P and using the result as our distance. Then, applying VICc we penalize connections and determine the correct network structure. A detailed version of the algorithm is found in Section 5.2.

10.3 Major Contribution 3: Matlab Toolbox for Robust Network Reconstruction

The third major contribution of this thesis is a Matlab Toolbox that implements the algorithm for robust reconstruction of networks with both diagonal and non-diagonal P. The Matlab Toolbox creates all possible combinations of Boolean structures and calculates α for each structure. The code then calculates $VICc$ values for each structure given their α values. Finally, the code finds the lowest $VICc$ value, and the associated structure becomes the

proposed structure for the network. Verification of the Matlab code can be found in Chapter 6.

10.4 Major Contribution 4: Applying Dynamical Structure Functions to Wireless Networks

In conjunction with the expansion of network reconstruction techniques associated with dynamical structure functions, we also developed theory to allow us to apply dynamical structure functions to wireless networks. This results was important because it shows how dynamical structure functions can be used beyond biological networks, for which purpose it was initially created.

There were two aspects of applying dynamical structure functions to wireless networks. First, the process was used to create a dynamic interference map while the network was online (Section 9.1) and, secondly, to use the dynamic map to determine whether intruders or other interfering devices were present within the network (Section 9.2).

10.5 Future Work: Theoretical Results

An interesting theoretical result to look at would be some way to tie the necessary and sufficient conditions developed in this thesis, which required G, to the robust results, which allowed us to reconstruct networks from data. Determining necessary and sufficient conditions directly from data would tie this together, but would require determining conditions on the input, u, and output, y, directly, which is much more complicated than determining under what conditions on G a network would be reconstructible.

As mentioned previously, we looked at the additive uncertainty on P, but it would be very interesting to look at additive uncertainty on Q or even additive uncertainty on both Q and P. Including Q in the additive uncertainty will represent the noise within the system more realistically.

Another possible theoretical result would be to apply dynamical structure functions to nonlinear systems. The current results only hold for linear time-invariant systems, so the only way to reconstruct nonlinear systems is to linearize them about an equilibrium. Developing results for reconstruction of nonlinear systems would greatly increase the applicability of dynamical structure functions.

For some applications, like biological networks, it is easier to perform experiments and collect data. For other applications, such as wireless networks, it is more difficult to ensure the network is in equilibrium in order to conduct experiments. Another interesting theoretical result would be to determine if the reconstruction of a network could be done using previously collected data rather than relying on the results of perturbation experiments.

Perhaps the most important theoretical result would probably be to improve the combinatoric search over all possible Boolean structures. Reducing this search to polynomial time has been attempted in [41], but this search currently has too many restrictions to make it applicable to a large number of networks.

10.6 Future Work: Applications

With regards to the specific applications discussed in this thesis, for biological networks, now that we have solid theoretical results and computer simulations, the next step is to perform network reconstruction on actual data provided by the biologists with which we currently collaborate.

Similarly, we would like to perform network reconstruction from actual data from wireless networks as well as trying to improve the network reconstruction process by determining how to reconstruct the network without a central controller. Currently, we need rate controllers to ensure that the system is in equilibrium and these controllers would need to be set by some sort of central controllers, it would be interesting to determine if we could determine the correct rates at which to send by using only local information as well as coordinating the perturbation experiments locally.

Finally, dynamical structure functions seem to lend themselves well to networks with fluid-like dynamics, such as biological systems and wireless networks. Another interesting application with a similar style of dynamics are social networks. The first step in applying dynamical structure functions to social networks would be to determine how to model them using differential equations in order to understand the notion of structure in those type of networks.

Chapter 11

References

[1] Y. Yuan, G. Stan, S. Warnick, and J. Goncalves, "Robust dynamical network reconstruction," *Automatica*, vol. 47:6, pp. 1230–1235, 2011.

[2] M. Andrec, B. Kholodenko, R. Levy, and E. Sontag, "Inference of signaling and gene regulatory networks by steady-state perturbation experiments: structure and accuracy," *Journal of Theoretical Biology*, vol. 232:3, pp. 427–441, 2005.

[3] T. Lenser, T. Hinze, B. Ibrahim, and P. Dittrich, "Towards evolutionary network reconstruction tools for systems biology," *Lecture Notes in Computer Science*, vol. 4447, pp. 132–142, 2007.

[4] E. Novikov and E. Barillot, "Regulatory network reconstruction using an integral additive model with flexible kernel functions," *BMC Systems Biology*, vol. 2:8, 2008.

[5] R. H. Dejan Stokic and S. Thurner, "A fast and efficient gene-network reconstruction method from multiple over-expression experiments," *BMC Bioinformatics*, vol. 10:253, 2009.

[6] S. Baginsky, L. Hennig, P. Zimmermann, and W. Gruissem, "Gene expression analysis, proteomics, and network discovery," *Plant Physiology*, vol. 152:2, pp. 402–410, 2010.

[7] Y. Zhou, J. Gerhart, and A. Sacan, "Reconstruction of gene regulatory networks by stepwise multiple linear regression from time-series microarray data," in *Proceedings of the International Symposium on Health Informatics and Bioinformatics*, pp. 76–81, 2012.

[8] B. Mlecnik, M. Tosolini, P. Charoentong, A. Kirilovsky, G. Bindea, A. Berger, M. Camus, M. Gillard, P. Bruneval, W. Fridman, F. Pages, Z. Trajanosk, and J. Galon, "Biomolecular network reconstruction identifies t-cell homing factors associated with survival in colorectal cancer," *Gastroenterology*, vol. 138:4, pp. 1429–1440, 2010.

[9] N. Duarte, S. Becker, N. Jamshidi, I. Thiele, M. Mo, T. Vo, R. Srivas, and B. Palssonr, "Global reconstruction of the human metabolic network based on genomic and bibliomic data," *Proceedings of the National Academy of Sciences*, vol. 104:6, pp. 1777–1782, 2007.

[10] R. Guthke, U. Mller, M. Hoffmann, F. Thies, and S. Topfe, "Dynamic network reconstruction from gene expression data applied to immune response during bacterial infection," *Bioinformatics*, vol. 21:8, pp. 1626–1634, 2005.

[11] D. Niculescu, "Interference map for 802.11 networks," in *Proceedings of the ACM SIGCOMM Conference on Internet Measurement*, pp. 339–350, 2007.

[12] B. Eriksson, G. Dasarathy, P. Barford, and R. Nowak, "Toward the practical use of network tomography for internet topology discovery.," in *Proceedings of the Conference on Information Communications*, pp. 1–9, 2010.

[13] Y. Qiao, G. Wang, X.-S. Qiu, and R. Gu, "Network loss tomography using link independence," in *Proceedings of the IEEE Symposium on Computers and Communications*, pp. 569–574, 2012.

[14] V. Chetty, D.Harbaugh, A. Rai, J. Wu, E. Vaziripour, S. Warnick, and D. Zappala, "Using signal structure to map and detect interference in wireless networks," in *submitted to the Conference on Information Communications 2012*.

[15] A. Papachristodoulou and B. Recht, "Determining interconnections in chemical reaction networks," in *Proceedings of the American Control Conference*, pp. 4872–4877, 2007.

[16] E. Sontag, "Lecture notes on mathematical systems biology." `http://www.math.rutgers.edu/~sontag/FTP_DIR/systems_biology_notes.pdf`, 2011.

[17] S. Berline and C. Bricker, "The law of mass action," *Journal of Chemical Education*, vol. 46:8, pp. 499–501, 1969.

[18] A. Hill, "The possible effects of the aggregation of the molecules of haemoglobin on its dissociation curves," *Journal of Physiology*, vol. 40, pp. iv–vii, 1910.

[19] S. Goutelle, M. Maurin, F. Rougier, X. Barbaut, L. Bourguignon, M. Ducher, and P. Maire, "The hill equation: a review of its capabilities in pharmacological modelling," *Fundamental & Clinical Pharmacology*, vol. 22:6, pp. 633–648, 2008.

[20] L. Michaelis, M. Menten, K. Johnson, and R. Goody, "The original Michaelis constant: translation of the 1913 Michaelis-Menten paper," *Biochemistry*, vol. 50:39, pp. 8264–8269, 2011.

[21] K. Astrom and R. Murray, *Feedback Systems: An Introduction for Scientists and Engineers*. Princeton University Press, 2008.

[22] J. Hespanha, *Linear Systems Theory*. Princeton University Press, 2009.

[23] H. Khalil, *Nonlinear Systems Third Edition*. Prentice Hall, Inc., 2002.

[24] J. Leigh, *Essentials of Nonlinear Control Theory, Volume 2*. Peter Peregrinus Ltd., 1983.

[25] J. Ramos, "Piecewise-linearized methods for oscillators with limit cycles," *Chaos, Solitons & Fractals*, vol. 27:5, pp. 1229–1238, 2006.

[26] E. Yeung, J. Gonçalves, H. Sandberg, and S. Warnick, "Representing structure in linear interconnected dynamical systems," in *Proceedings of the Conference on Decision and Control*, pp. 6010–6015, 2010.

[27] W. Zheng, "A least-squares based algorithm for transfer function identification," in *Proceedings of the International Symposium on Signal Processing and its Applications*, vol. 1, pp. 183–186, 1999.

[28] J. Gonçalves and S. Warnick, "Necessary and sufficient conditions for dynamical structure reconstruction of LTI networks," *IEEE Transactions on Automatic Control*, vol. 53:7, pp. 1670–74, 2008.

[29] D. Marbacha, R. Prillc, T. Schafftera, C. Mattiussia, D. Floreanoa, and G. Stolovitzkyc, "Revealing strengths and weaknesses of methods for gene network inference," in *Proceedings of the National Academy of Sciences*, vol. 107:14, pp. 6286–6291, 2010.

[30] F. Galton, "Co-relations and their measurement," in *Proceedings of the Royal Society*, vol. 45, pp. 135–145, 1888.

[31] J. Rice, Y. Tu, and G. Stolovitzky, "Reconstructing biological networks using conditional correlation analysis," *Bioinformatics*, vol. 21:6, pp. 765–773, 2005.

[32] A. Arkin, P. Shen, and J. Ross, "A test case of correlation metric construction of a reaction pathway from measurements," *Science*, vol. 277:5330, pp. 1275–1279, 1997.

[33] J. Aldrich, "Correlations genuine and spurious in pearson and yule," *Statistical Science*, vol. 10:4, pp. 364–376, 1995.

[34] E. Neto, C. Ferrara, A. Attie, and B. Yandell, "Inferring causal phenotype networks from segregating populations," *Genetics*, vol. 179:2, pp. 1089–1100, 2008.

[35] F. Ruggeri, F. Faltin, and R. Kenett, *Encyclopedia of Statistics in Quality & Reliability*. Wiley & Sons, 2007.

[36] N. Friedman, "Inferring cellular networks using probabilistic graphical models," *Science*, vol. 303, pp. 799–805, 2004.

[37] G. Quer, H. Meenakshisundaram, B. Tamma, B. Manoj, R. Rao, and M. Zorzi, "Using Bayesian networks for cognitive control of multi-hop wireless networks," pp. 201–206, 2010.

[38] D. Madigan, W.-H. Ju, P. Krishnan, A. Krishnakumar, and I. Zorych, "Location estimation in wireless networks: A Bayesian approach," *Statistica Sinista*, vol. 16:2, pp. 495–522, 2006.

[39] S. Kim, S. Imoto, and S. Miyano, "Inferring gene networks from time series microarray data using dynamic Bayesian networks," *Briefings in Bioinformatics*, vol. 4:3, pp. 228–235, 2003.

[40] N. Friedman, K. Murphy, and S. Russell, "Learning the structure of dynamic probabilistic networks," in *Proceedings of the Conference on the Uncertainty in Artificial Intelligence*, pp. 139–147, 1998.

[41] D. Hayden, Y. Yuan, and J. Goncalves, "Robust reconstruction in polynomial time," in *accepted to the Conference on Decision and Control 2012.*

[42] J. Tegner, M. Yeung, J. Hasty, and J. Collins, "Reverse engineering gene networks: Integrating genetic perturbations with dynamical modeling," in *Proceedings of the National Academy of Sciences*, vol. 100, pp. 5944–5949, 2003.

[43] S. Li, S. Assmann, and R. Albert, "Predicting essential components of signal transduction networks: A dynamic model of guard cell abscisic acid signaling," *PLoS Biology*, vol. 4:10, p. e312, 2006.

[44] R. Bonneau, D. Reiss, P. Shannon, M. Facciotti, L. Hood, N. Baliga, and V. Thorsson, "The inferelator: an algorithm for learning parsimonious regulatory networks from systems-biology data sets de novo," *Genome Biology*, vol. 7:5, pp. 1–16, 2006.

[45] A. Julius, M. Zavlanos, S. Boyd, and G. Pappas, "Genetic network identification using convex programming," *IET Systems Biology*, vol. 3, pp. 155–166, 2009.

[46] B. Wilczynski and J. Tiury, "Regulatory network reconstruction using stochastic logical networks," in *Proceedings of the International Conference on Computational Methods in Systems Biology*, pp. 142–154, 2006.

[47] C. Beck, J. Doyle, and K. Glover, "Model reduction of multidimensional and uncertain systems," *IEEE Transactions on Automatic Control*, vol. 41:10, pp. 1466–1477, 1996.

[48] H. Sandberg and R. Murray, "Frequency-weighted model reduction with applications to structured models," in *Proceedings of the American Control Conference*, pp. 941–946, 2007.

[49] E. Yeung, J. Goncalves, H. Sandberg, and S. Warnick, "Network structure preserving model reduction with weak a priori structural information," in *Proceedings of the Conference on Decision and Control*, pp. 3256–3263, 2009.

[50] A. Aswani and C. Tomlin, "Reachability algorithm for biological piecewise-affine hybrid systems," *Lecture Notes in Computer Science*, vol. 4416, pp. 633–636, 2007.

[51] P. Iglesias and B. Ingalls, *Control Theory and Systems Biology*. MIT Press, 2010.

[52] H. Kitano, "Computational systems biology," *Nature*, vol. 420:6912, pp. 206–210, 2002.

[53] R. de Oliveira and T. Braun, "A dynamic adaptive acknowledgment strategy for TCP over multihop wireless networks," in *Proceedings of the Conference on Information Communications*, vol. 3, pp. 1863–1874, 2005.

[54] Z. Fu, P. Zerfos, H. Luo, S. Lu, L. Zhang, and M. Gerla, "The impact of multihop wireless channel on TCP throughput and loss," in *Proceedings of the Conference on Information Communications*, vol. 3, pp. 1744–1753, 2003.

[55] T. Nandagopal, T.-E. Kim, X. Gao, and V. Bharghavan, "Achieving MAC layer fairness in wireless packet networks," in *Proceedings of the International Conference on Mobile Computing and Networking*, pp. 87–98, 2000.

[56] J. Padhye, S. Agarwal, V. Padmanabhan, L. Qiu, A. Rao, and B. Zill, "Estimation of link interference in static multi-hop wireless networks," in *Proceedings of the ACM SIGCOMM Conference on Internet Measurement*, pp. 305–310, 2005.

[57] Y. Li, L. Qiu, Y. Zhang, R. Mahajan, and E. Rozner, "Predictable performance optimization for wireless networks," in *Proceedings of the ACM SIGCOMM Conference on Data Communication*, pp. 413–426, 2008.

[58] T. Salonidis, G. Sotiropoulos, R. Guerin, and R. Govindan, "Online optimization of 802.11 mesh networks," in *Proceedings of the International Conference on Emerging Networking Experiments and Technologies*, pp. 61–72, 2009.

[59] C. Reis, R. Mahajan, M. Rodrig, D. Wetherall, and J. Zahorjan, "Measurement-based models of delivery and interference in static wireless networks," in *Proceedings of the Conference on Applications, Technologies, Architectures, and Protocols for Computer Communications*, pp. 51–62, 2006.

[60] K.-Y. Jang, M. Carrera, K. Psounis, and R. Govindan, "Passive on-line in-band interference inference in centralized WLANs." Technical Report, Department of Computer Science, University of Southern California.

[61] V. Shrivastava, S. Rayanchu, S. Banerjee, and K. Papagiannaki, "PIE in the sky: online passive interference estimation for enterprise WLANs," in *Proceedings of the Conference on Networked Systems Design and Implementation*, p. 25, 2011.

[62] K. Cai, M. Blackstock, M. J. Feeley, and C. Krasic, "Non-intrusive, dynamic interference detection for 802.11 networks," in *Proceedings of the ACM SIGCOMM Conference on Internet Measurement*, pp. 377–383, 2009.

[63] N. Ahmed, U. Ismail, S. Keshav, and K. Papagiannaki, "Online estimation of RF interference," in *Proceedings of the International Conference on Emerging Networking Experiments and Technologies*, pp. 4:1–4:12, 2008.

[64] L. Ljung, *System Identification: Theory for the User*. Prentice Hall, 1987.

[65] K. Zhou, J. Doyle, and K. Glover, *Robust and Optimal Control*. Prentice Hall, 1995.

[66] N. Young, *An Introduction to Hilbert Space*. Cambridge University Press, 1988.

[67] A. Hirotugu, "A new look at the statistical model identification," *IEEE Transactions on Automatic Control*, vol. 19:6, pp. 716–723, 1974.

[68] K. Burnham and D. Anderson, *Model Selection and Inference: A Practical Information-Theoretic Approach*. Springer-Verlag, 1998.

[69] J. Goncalves, R. Howes, and S. Warnick, "Dynamical structure function for the reverse engineering of LTI networks," in *Proceedings of the Conference on Decision and Control*, pp. 1516–1522, 2007.

[70] M. Plesinger, *The Total Least Squares Problem and Reduction of Data in $AX \approx B$*. PhD Thesis, 2008.

[71] F. Semplici, M. Vaxillaire, S. Fogarty, M. Semache, A. Bonnefond, G. Fontes, J. Philippe, G. Meur, F. Diraison, R. Sessions, J. Rutter, V. Poitout, P. Froguel, and G. Rutter, "Human mutation within Per-Arnt-Sim (PAS) domain-contaning protein kinase (PASK) causes basal insulin hypersection," *Journal of Biological Chemistry*, vol. 286:51, pp. 44005–44014, 2011.

[72] C. Kikani, S. Antonysamy, J. Bonanno, R. Romero, F. Zhang, M. Russell, T. Gheyi, M. Iizuka, S. Emtage, J. Sauder, B. Turk, S. Burley, and J. Rutter, "Structural bases of PAS domain-regulated kinase (PASK) activation in the absence of activation loop phosphorylation," *The Journal of Biological Chemistry*, vol. 285:52, pp. 41034–41043, 2010.

[73] J. Rutter, B. Probst, and S. McKnight, "Coordinate regulation of sugar flux and translation by PAS kinase," *Cell*, vol. 111:1, pp. 17–28, 2002.

[74] T. Smith and J. Rutter, "Regulation of glucose partitioning by PAS kinase and Ugp1 phosphorylation," *Molecular Cell*, vol. 26:4, pp. 491–499, 2007.

[75] J. Grose, T. Smith, H. Sabic, and J. Rutter, "Yeast PAS kinase coordinates glucose partitioning in response to metabolic and cell integrity signaling," *The European Molecular Biology Organization*, vol. 26:23, pp. 4824–4830, 2007.

Chapter 12

Appendix

Function 1: createDiag

```
function [Qcoff, Qstruct, Pcoff, Pstruct, count1, count2] = createDiag(N)

N = ceil(N);
% Check to ensure input is positive
if N < 1
    error('You must provide a positive number')
end

% A priori information, the structure of Q and P
Qcoff = cell(N,N);
Qstruct = cell(N,N);

Pcoff = cell(N,N);
Pstruct = cell(N,N);

count1 = 0;
count2 = 0;

for i = 1:N
    for j = 1:N
        if i ~= j
            % Place 1 in each offdiagonal of Qcoff and increasing numbers
            % in each offdiagonal of Qstruct
            count1 = count1 + 1;
            Qcoff{i,j} = 1;
            Qstruct{i,j} = count1;
```

```
            Pcoff{i,j} = 0;
            Pstruct{i,j} = 0;
        else
            % Place 1 in each diagonal of Pcoff and increasing numbers in
            % each diagonal of Pstruct
            count2 = count2 + 1;
            Pcoff{i,j} = 1;
            Pstruct{i,j} = count2;

            Qcoff{i,j} = 0;
            Qstruct{i,j} = 0;
        end
    end
end
```

Function 2: findT

```
function T = findT(Qcoff, Pcoff, Qstruct, Pstruct, c1, c2)
% Variables
[r,s] = size(Qcoff);
[u,v] = size(Qstruct);
[w,~] = size(Pcoff);
[c,~] = size(Pstruct);

% Ensure that Qcoff and Qstruct are square and same size
if r ~= s
    error('Qcoff must be a square matrix');
end
if u ~= v
    error('Qstruct must be a square matrix');
end
if u ~= r
    error('Qcoff and Qstruct must be the same dimensions');
end
```

```
% Ensure that Pcoff and Pstruct are the same size and have the same number
% of rows as Q
if w ~= c
    error('Pcoff and Pstruct must be the same dimensions');
end
if w ~= r
    error('Pcoff and Pstruct must have the same number of
    rows as Qcoff and Qstruct');
end

% Make sure Q has zeros on the diagonal
for i = 1:r
    if Qcoff{i,i} ~= 0 | Qstruct{i,i} ~= 0
        error('Q structure contains non-zero diagonal values.');
    end
end

% Stack the a priori information into a vector
q1 = vectorizeCell(Qstruct);
p1 = vectorizeCell(Pstruct);

q2 = vectorizeCell(Qcoff);
p2 = vectorizeCell(Pcoff);

% Create the part of T that affects Q
[a,~] = size(q1);
T1 = zeros(a, c1);
cut = 0;
for i = a:-1:1
    % Ensure that the cell sizes of Qcoff and Qstruct are the same
    if size(q1{i}) ~= size(q2{i})
        error('Cell sizes must be the same in Qcoff and Qstruct');
    end
    for j = 1:size(q1{i})
        % Qstruct tells us which rows are affected
```

```
        if q1{i,j} ~= 0
            % Qcoff tells us by how much
            T1(i,q1{i,j}) = q2{i,j};
        end
    end
end

% Create the part of T that affects P
[b,~] = size(p1);
T2 = zeros(b, c2);
for i = 1:b
    % Ensure that the cell sizes of Pcoff and Pstruct are the same
    if size(p1{i}) ~= size(p2{i})
        error('Cell sizes must be the same in Pcoff and Pstruct');
    end
    for j = 1:size(p1{i})
        % Pstruct tells us which rows are affected
        if p1{i,j} ~= 0
            % Pcoff tells us by how much
            T2(i,p1{i,j}) = p2{i,j};
        end
    end
end

% Create T by making the block diagonal matrix [T1 0; 0 T2];
T = [T1 zeros(a-cut,c2); zeros(b,c1) T2];
```

Function 3: robustRecon

```
function [Q,P] = robustrecon(T, y, u, N, C, displ)
% Find delta for every possible boolean structure
aalphas = findAlphas(T, y, u, N);

% Given all deltas, use AICc to determine the correct structure for Q
bestX = findBest(aalphas, N, displ, y);
```

```
% From previous information, find the Boolean structure of P and Q
P = findP(T,C,y,u);
Q = findQ(T,N,y,bestX);
```

Function 4: findAlphas

```
function aalphas = findAlphas(T, y, u, N)

% Find all possible Boolean structures
allX = findCombs(N);
[h,~] = size(allX);

% Variables
aalpha = zeros(2^N,1+N);
count = 1;

% For each boolean structure, find alpha and store in aalpha
for i = 1:h
    alpha = getAlpha(T, y, u, allX{i});
    aalpha(count,:) = [alpha vectorize(allX{i})'];
    count = count + 1;
end

% Sort structures by alpha values
aalphas = sortrows(aalpha, -1);
```

Function 5: findCombs

```
function allX = findCombs(N)
N = ceil(N);
% Ensure N is positive
if N < 1
    error('You must enter a positive number.')
end
% Find number of possible combinations
```

```
p = 2^(N);
for i = 0:p-1
    % For each number, find the binary value
    str = dec2bin(i);
    [~,k] = size(str);
    % Convert binary value to an array
    x = zeros(1,N);
    count = k;
    for m = N:-1:1
        x(1,m) = str2double(str(1,count));
        count = count - 1;
        if count <= 0
            break
        end
    end
    % Store binary array in matrix
    allX{i+1,1} = x; %#ok<AGROW>
end
```

Function 6: getAlpha

```
function alpha = getAlpha(T, y, u, X)
% Find x number of points on the unit circle, where x = numPoints
numPoints = 10;
t = linspace(0,2*pi,numPoints);
a = cos(t);
b = sin(t);
alpha = 0;

% For each point on the unit circle, find the score of XY-U
for c = 1:numPoints
    % Find the Z-transform of Y and U
    z = a(c)+1i*b(c);
    Y = zTransform(y, z);
    U = zTransform(u, z);
```

```
    % Find Mx = vecY, where x is the vector of unknowns
    M = findM(Y,U);
    M = M*T;

    % Remove columns in M that correspond to zeros in the current Boolean
    % structure
    x = vectorize(X);
    [d,~] = size(x);
    for i = d:-1:1
        if x(i,1) == 0
            M(:,i) = [];
        end
    end

    % Use total least squares (or least squares) to determine delta for the
    % current point
    alphaNow = solveAlpha(M,Y);

    % Find the largest delta value from all the points on the unit circle
    if alphaNow > alpha
        alpha = alphaNow;
    end
end
```

Function 7: zTransform

```
function X = zTransform(x, z)
% Calculate the Z-transform of x at the point z
[row,col] = size(x);
X = zeros(row,col);
for i = 1:row
    for j = 1:col
        [m,~] = size(x{i,j});
        for k = 1:m
```

```
            % Equation for finite Z-transform
            X(i,j) = X(i,j) + x{i,j}(k,1)*z^-(k-1);
        end
    end
end
```

Function 8: findM

```
function M = findM(Y,U)
% Variables
[q,r] = size(Y);
Z = zeros(r,q);

% Create blockdiag(Y', Y', ..., Y')
X = [];
for j = 1:r
    for i = 0:(j-2)
        X = [X Z];
    end
    X = [X Y.'];
    for i = j:(r-1)
        X = [X Z];
    end
    if j == 1
        D = X;
    else
        D = [D;X];
    end
    X = [];
end

% Create blockdiag(U', U', ..., U')
[q,r] = size(U);
Z = zeros(r,q);
X = [];
```

```
for j = 1:r
    for i = 0:(j-2)
        X = [X Z];
    end
    X = [X U.'];
    for i = j:(r-1)
        X = [X Z];
    end
    if j == 1
        B = X;
    else
        B = [B;X];
    end
    X = [];
end

% Append D and B to get M (without columns removed for zeros in Q)
M = [D B];
```

Function 9: vectorize

```
function v = vectorize(M)
% Stacks each row of M into the vector v
[p,m] = size(M);
v = zeros(1, p*m);
count = 1;
for i = 1:p
    for j = 1:m
    v(1, count) = M(i,j);
    count = count + 1;
    end
end
v = v';
```

Function 10: vectorizeCell

```
function v = vectorizeCell(M)
% Stacks each row of M into the vector v
[p,m] = size(M);
v = cell(1, p*m);
count = 1;
for i = 1:p
    for j = 1:m
    v(1, count) = M(i,j);
    count = count + 1;
    end
end
v = v';
```

Function 11: solveAlpha

```
function a = solveAlpha(M, Y)
% Use total least squares to find the vector of unknowns
vecY = vectorize(Y);
solX = pinv(M)*vecY;
% Use the 2-norm squared to solve for alpha
a = norm(M*solX-vecY);
a = a'*a;
```

Function 12: findBest

```
function bestX = findBest(aalphas, N, displ,y)
% Variables
score = intmax;
bestX = zeros(1,N);
[q,~] = size(aalphas);

% For each boolean structure, given alpha, calculate VIC and VICc
for j = 1:q
```

```
    % Count number of nonzero values in current Boolean structure
    L = numNonZero(aalphas(j,2:1+N));
    [e,~] = size(y);
    % Calculate VIC and VICc
    [a1,a2] = vicc(aalphas(j,1),L,e);
    aalphas(j,N+2:N+3) = [a1,a2];
    % Display results if flag is set
    if displ == 1
        disp([mat2str(aalphas(j,2:1+N)) ' alpha = '
        mat2str(aalphas(j,1),4) ', VIC = '
        mat2str(aalphas(j,N+2),4) ', VICc = '
        mat2str(aalphas(j,N+3),4)])
    end
    % Determine the structure with the current lowest score
    if a2 < score
        score = a2;
        bestX = aalphas(j,2:1+N);
    end
end
```

Function 13: numNonZero

```
function N = numNonZero(V)

% Variables
[n,m] = size(V);
N = 0;

% Count number of nonzero values in matrix V
for i = 1:n
    for j = 1:m
        if V(i,j) ~= 0
            N = N + 1;
        end
    end
end
```

Function 14: vicc

```
% Vasu's Information Criterion
function [vic,vicc] = vicc(alpha, L, N)

% Returns vasu's scores (VIC and VICc)
vic = 10*L + alpha;
vicc = vic + 10*L*(L+1)/(N*N-L-1);
```

Function 15: findP

```
function P = findP(T,C,y,u)
% Variables
[a,b] = size(T);
[p,~] = size(y);
[m,~] = size(u);
T = T(a-p*m+1:a,b-C+1:b);
P = zeros(p,m);
[a,~] = size(T);
% Go through the rows of T corresponding to P, if it is non-zero place in
% the same row as T
for i = 1:a
    for j = 1:C
        if T(i,j) ~= 0
            n = mod(i,C);
            if n == 0
                n = C;
            end
            P(ceil(i/p),n) = 1;
        end
    end
end
```

Function 16: findQ

```
function Q = findQ(T,N,y,bestX)
% Variables
[a,b] = size(T);
[p,~] = size(y);
T = T(1:p^2,1:N);
Q = zeros(p,p);
[a,~] = size(T);
% Go through the rows of T corresponding to P, if it is non-zero place in
% the same row as T
count = 1;
for i = 1:a
    for j = 1:N
        if T(i,j) ~= 0
            n = mod(i,p);
            if n == 0
                n = p;
            end
            Q(ceil(i/p),n) = bestX(1,count);
            count = count + 1;
        end
    end
end
```